2017

Quantifying Carbonyl Sulfide and Other Sulfur-Containing Compounds Over the Santa Barbara Channel

Julia Black
Scripps College

Quantifying Carbonyl Sulfide and Other Sulfur-Containing Compounds Over the Santa Barbara Channel

A Thesis Presented

by

Julia Black

To the Keck Science Department

Of Claremont Mckenna, Pitzer, and Scripps College

In partial fulfillment of

The degree of Bachelor of Arts

Senior Thesis in Environmental Science

December 2016

Table of Contents

ABSTRACT

Carbonyl sulfide (OCS) is emitted to the atmosphere through the outgassing of ocean surface waters. OCS is also the primary source of sulfur-containing compounds in the stratosphere and contributes to the formation of the stratospheric sulfate layer, an essential controller of the radiative balance of the atmosphere. During the 2016 Student Airborne Research Program (SARP), 15 whole air samples were collected on the NASA DC-8 aircraft over the Santa Barbara Channel. Five additional surface samples were taken at various locations along the Santa Barbara Channel. The samples were analyzed using gas chromatography in the Rowland-Blake lab at UC Irvine, and compounds associated with ocean emissions including OCS, dimethyl sulfide (DMS), carbon disulfide (CS_2), bromoform ($CHBr_3$), and methyl iodide (CH_3I) were examined. Excluding OCS, the vertical distribution of marine tracers that were analyzed showed dilution with increasing altitude. For OCS, the surface samples all exhibited elevated concentrations of OCS in comparison to samples taken from the aircraft, with an average of 666 ± 26 pptv, whereas the average concentration of OCS in the aircraft samples was 581 ± 9 pptv. 2016 Surface samples were compared to surface samples from SARP campaigns between 2009-2015 taken near or within the 2016 study region. The 2009-2015 samples exhibited an average OCS concentration of 526 ± 8 pptv. It is evident that the 2016 surface samples measured higher concentrations of OCS than ever recorded during previous SARP campaigns and in comparison to global averages: 525 ± 17 pptv in the Northern hemisphere and 482 ± 13 pptv in the Southern hemisphere (Sturges et al., 2001). OCS emissions should be measured using surface samples if emission estimates from the ocean are to be evaluated since measurements from the aircraft (500 ft) are not sufficiently capturing surface concentrations. Additionally, OCS enhancements seen in 2016 had never before been detected by surface samples, revealing a potential phenomenon at work causing the elevation during this year's campaign.

INTRODUCTION

On a global scale, carbonyl sulfide (OCS) is the most abundant sulfur-containing trace gas species in the atmosphere, with an average global mixing ratio of 500 parts per trillion by volume (pptv) and a relatively long atmospheric lifetime of 2-7 years (Xu et al., 2001). It is derived via the atmospheric oxidation of dimethyl sulfide (DMS) through a presently unknown mechanism (Arsene et al., 1999), and via oxidation of carbon disulfide (CS_2) shown in equation 1:

$$OH + CS_2 \rightarrow OCS + HS \qquad (1)$$

where a reaction initiated by an OH radical occurs with CS_2 to produce OCS and sulfanyl, a radical molecule made up of one hydrogen and one sulfur atom (Sze & Ko, 1980). OCS is also derived from the photolysis of CS_2 as shown in equation 2:

$$CS_2 + h\nu \rightarrow OCS + CO + SO_2 \qquad (1)$$

where OCS, carbon monoxide (CO) and sulfur dioxide (SO_2) are produced (Sze & Ko, 1980).

Emissions of Sulfur Compounds

Nearly half of atmospheric OCS is a result of direct and indirect emissions from the ocean (Kettle, 2002; Commane et al., 2013). Direct emissions stem from ocean areas of high biological productivity where OCS is produced photochemically from biogenic organosulfur compounds in the marine euphotic zone (Andreae & Ferek, 1992; Xu et al., 2001; Svoronos & Bruno, 2002). Surface waters, coastal, and shelf regions are the dominant areas for ocean emissions of OCS, being up to ten times higher than concentrations in the open ocean (Andreae & Ferek, 1992). Indirect emissions are produced via the oxidation of DMS and CS_2 as shown in equation 1 (Crutzen, 1976). With the recognition that ocean surface waters are generally supersaturated with OCS, it is understood that oceans release sulfur gases into the atmosphere, and are ultimately large contributors to the atmospheric budget of OCS (Bruhl et al., 2012; Launois et al., 2015). OCS is also released to the atmosphere via biomass burning, anoxic soils, wetlands, and volcanism, and is removed by uptake from terrestrial vegetation, soil, photolysis, and reactions with OH and O radicals (Watts, 2000; Blake et al., 2004; Brühl et al., 2012; Commane et al., 2013).

DMS and CS_2 are also produced in the surface waters of the upper ocean and are outgassed to the atmosphere where they are oxidized into gaseous sulfur-species, including OCS (Barnes, Becker, & Patroescu, 1994; Kettle et al., 2002). DMS is the most abundant biological sulfur-containing compound in the atmosphere, derived from the primary production of marine phytoplankton and through complex biological cycling (Keller et al., 1989). DMS is present due to its release along with its precursor, dimethylsulfoniopropionate (DMSP), by phytoplankton to regulate the osmotic pressure of their cells (Jodwalis et al., 2000). It is also sourced from salt-marshes and estuaries, soils, tropical forests, and vegetation (Watts, 2000). CS_2, in addition to being produced in the ocean surface layer, can also be sourced from anoxic soils, photochemical reactions, microbial processes in wetlands, and volcanic eruptions (Khalil & Rasmussen, 1984).

A table summarizing the sources of the previously described sulfur-containing compounds is provided below:

Table 1. Summary of the main natural sources of OCS, DMS, and CS_2.

Species	Natural Sources
OCS	Ocean surface layer Biomass burning Oxidation of DMS and CS_2 Volcanic eruptions
DMS	Ocean surface layer Marine phytoplankton Marshes and estuaries Vegetation and soils Tropical forests
CS_2	Ocean surface layer Photochemical reactions Microbial processes Volcanic eruptions

OCS as a Source of Stratospheric Sulfate Aerosols

Due to its chemically inert state in the troposphere, the majority of tropospheric OCS persists long enough to be transported to the stratosphere where it is oxidized into sulfuric acid and condensed into stratospheric aerosols (Crutzen, 1976; Chin & Davis, 1995; Blake et al., 2008) as shown in equation 3:

$$OCS + h\nu \rightarrow CO + S(^1D) \qquad \lambda < 289.5 \text{ nm} \qquad (3\text{-I})$$

$$OCS + h\nu \rightarrow CO + S(^1S) \qquad \lambda < 210.5 \text{ nm} \qquad (3\text{-II})$$

$$S + O_2 \rightarrow SO + O \qquad (3a)$$

$$S + O_3 \rightarrow SO + O_2 \qquad (3b)$$

$$SO + O_2 \rightarrow SO_2 + O \qquad (3c)$$

$$SO_2 + OH \rightarrow HOSO_2 \qquad (3d)$$

$$HOSO_2 + O_2 \rightarrow HO_2 + SO_3 \qquad (3e)$$

$$SO_3 + H_2O \rightarrow H_2SO_4 \qquad (3f)$$

The mechanism of OCS loss is dominated by the photodissociation of OCS, reaction (I-II), which is the rate determining step of the reaction sequence. Atomic sulfur from the photodissociation of OCS forms sulfur monoxide (SO) in reactions (3a) and (3b), with the generation of SO_2 and sulfuric acid (H_2SO_4) in reactions (3c) through (3f) (Jacobson, 2005; Calvert et al., 2015).

Brühl et al. (2012) discuss how volcanoes are the main contributors to the stratospheric aerosol layer, but during volcanically quiescent periods, the conversion of OCS into H_2SO_4 is the dominant contributor to the presence of a thin stratospheric aerosol layer. This layer of sulfate aerosols is highly effective at reflecting incoming solar radiation back to space and thus enhances the Earth's albedo (Figure 1) (Charlson et al., 1990; Blake et al., 2008).

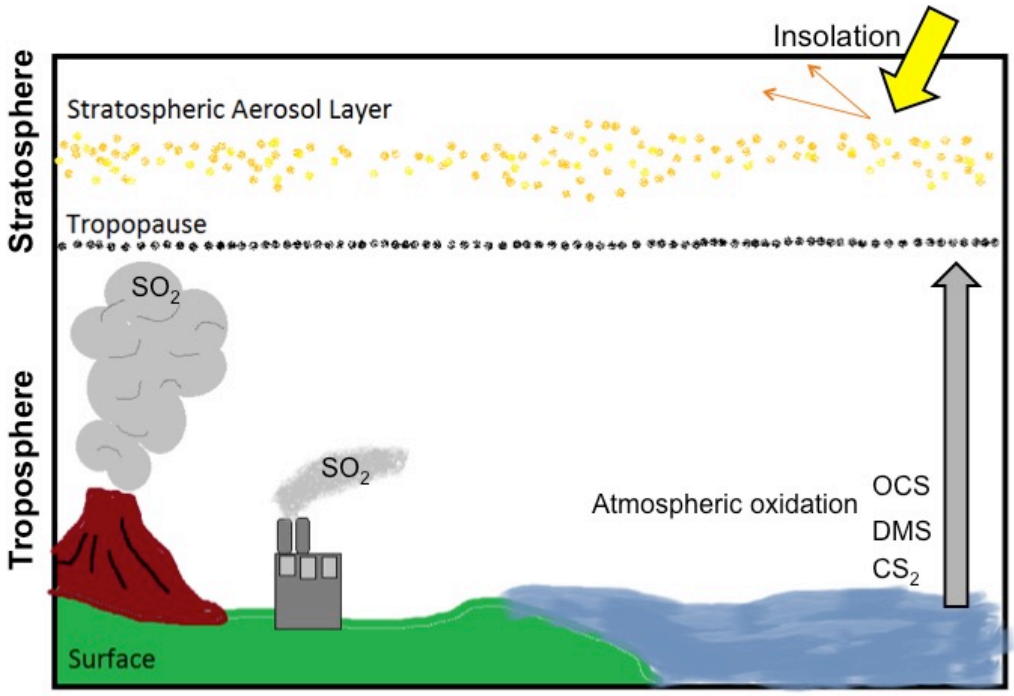

Figure 1. Diagram illustrating the transfer of OCS from the troposphere to the stratosphere where it is then oxidized into H_2SO_4 and condensed into stratospheric aerosols, creating a layer that is able to reflect incoming solar radiation back to space (Blake et al., 2008; created by Julia Black).

Radiative forcing, a measure of how the energy balance of the Earth-atmosphere system is influenced when climate-related factors are altered, has both natural and anthropogenic constituents as illustrated in figure 2 (Forster et al., 2007). This energy balance controls Earth's surface temperature and refers to the balance between incoming solar radiation and outgoing infrared radiation in Earth's atmosphere (Forster et al., 2007). It is thus important to understand natural emissions of OCS and other sulfur-containing compounds as natural climate coolers that cause a negative radiative forcing as aerosols, while simultaneously recognizing that anthropogenic-sourced sulfur emissions are "cooling" the planet at a substantial price.

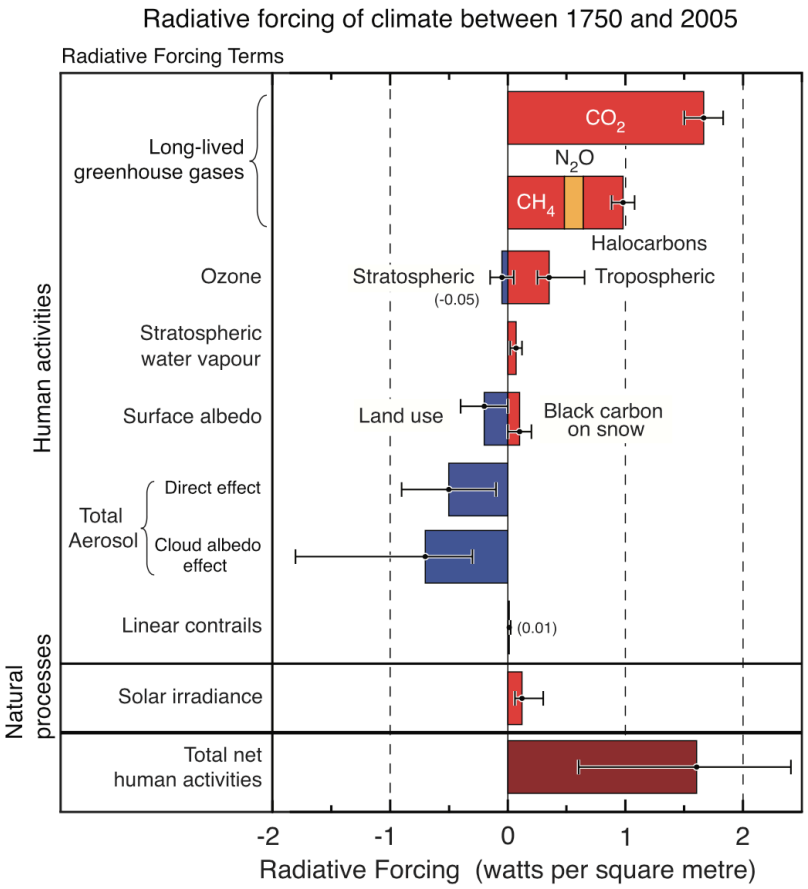

Figure 2. Summary of the main components of radiative forcing of climate change associated with natural processes or human activities (Forster et al., 2007).

Objectives of the Study

The purpose of this study is to analyze and compare concentrations of compounds associated with ocean emissions and stratospheric aerosols including OCS, DMS, CS_2, bromoform ($CHBr_3$), and methyl iodide (CH_3I). A further objective is to compare concentrations and sampling altitudes for samples collected over the Santa Barbara Channel. OCS is the main compound being analyzed for this study with the inclusion of other marine-sourced compounds for general profile comparison.

METHODS

Air samples were collected onboard the NASA DC-8 and at various surface locations on the Santa Barbara Channel during the Student Airborne Research Program (SARP) in June, 2016. Funded by the National Suborbital Education and Research Center (NSERC), SARP utilizes NASA's flying laboratories to expose undergraduate students to airborne science, providing participants with the opportunity to experience a scientific research campaign. Students assist in instrument operations onboard the aircraft to take whole air samples as well as to image the Earth's surface. A fleet of aircraft, including the DC-8 and ER-2, are used for studying Earth system processes. Whole air samples were collected on the DC-8 on June 18th, 2016, with additional samples taken on the Santa Barbara Channel from a dive boat on June 21st, 2016. Similar methods were used for past SARP campaigns, with data collection occurring on or near the same days as the 2016 SARP campaign.

Study Region

Research flights for this study were based out of the NASA Armstrong Flight Research Center in Palmdale, California. The research flight for this study on June 18th, 2016, focused on the San Joaquin Valley, flying over agricultural regions and cities in the Central Valley including Bakersfield, Fresno, and Merced, and over the Santa Barbara Channel (Figure 3). The focus region for this study was constrained to data collected over the Santa Barbara Channel and from samples obtained at the ocean surface from a dive boat. Samples over the study region from the first flight on June 17th, 2016 were excluded due to the presence of the Sherpa brush fire that burned in the Santa Ynez Mountains in Santa Barbara County because OCS, the main compound examined in this study, is also associated with biomass burning (Blake et al., 2004). The data were constrained between

the longitudes of 119° 56' 24" W and 119° 55' 12" W, and between the latitudes of 34° 25' 48" N and 34° 13' 12" N as shown in figure 6.

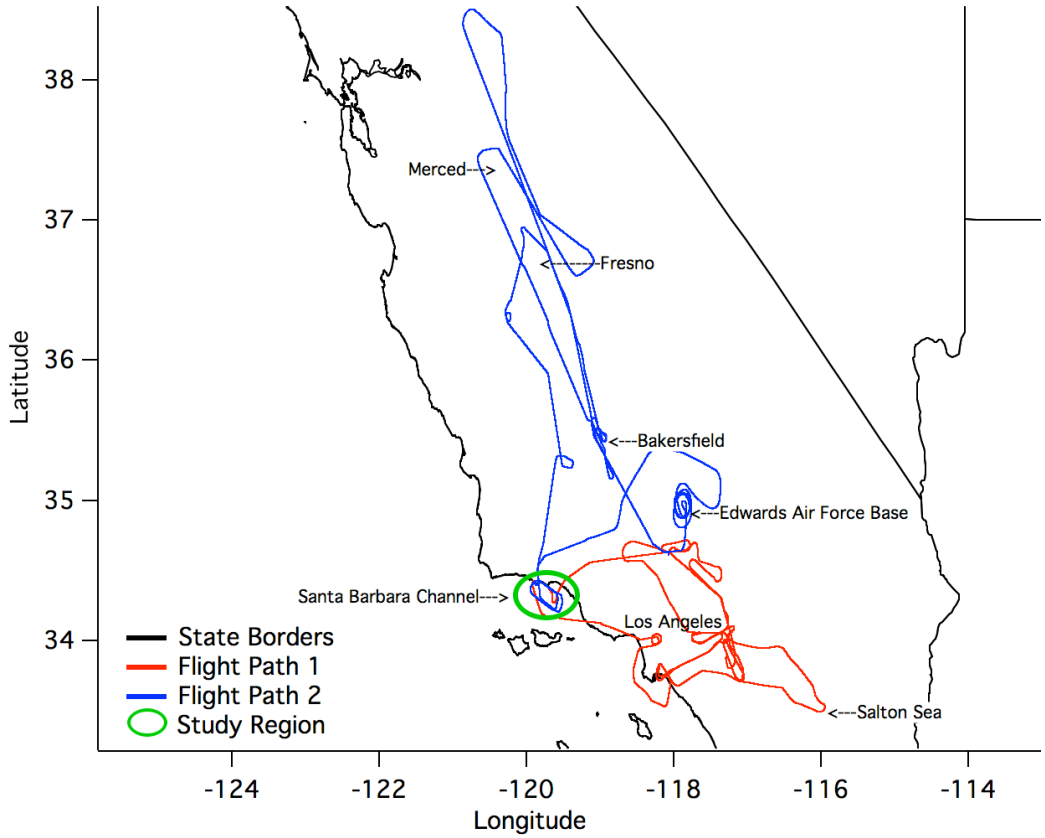

Figure 3. The full geographic range of the research flights conducted during the 2016 NASA SARP campaign in June, with the region of focus circled in green.

Data Collection

Using the University of California, Irvine's whole air sampler instrument, whole air samples were collected onboard the DC-8 at 1-8 minute intervals depending on the aircraft's altitude and position in relation to various sources of pollutants (Figure 4). For each sample, unfiltered air entered the aircraft from the outside through an air inlet using a dual bellows pump. An evacuated, 2-L stainless steel canister equipped with a bellows valve was then filled to a pressure of 40 psi by opening the canister valve and allowing it to fill for about 45 seconds. More than 220 canister samples were collected during the two research flights (Figure 5).

Figure 4. UCI Whole Air Sampler instrument onboard the DC-8 aircraft (left) and a view of the modified DC-8 with intake probes (right).

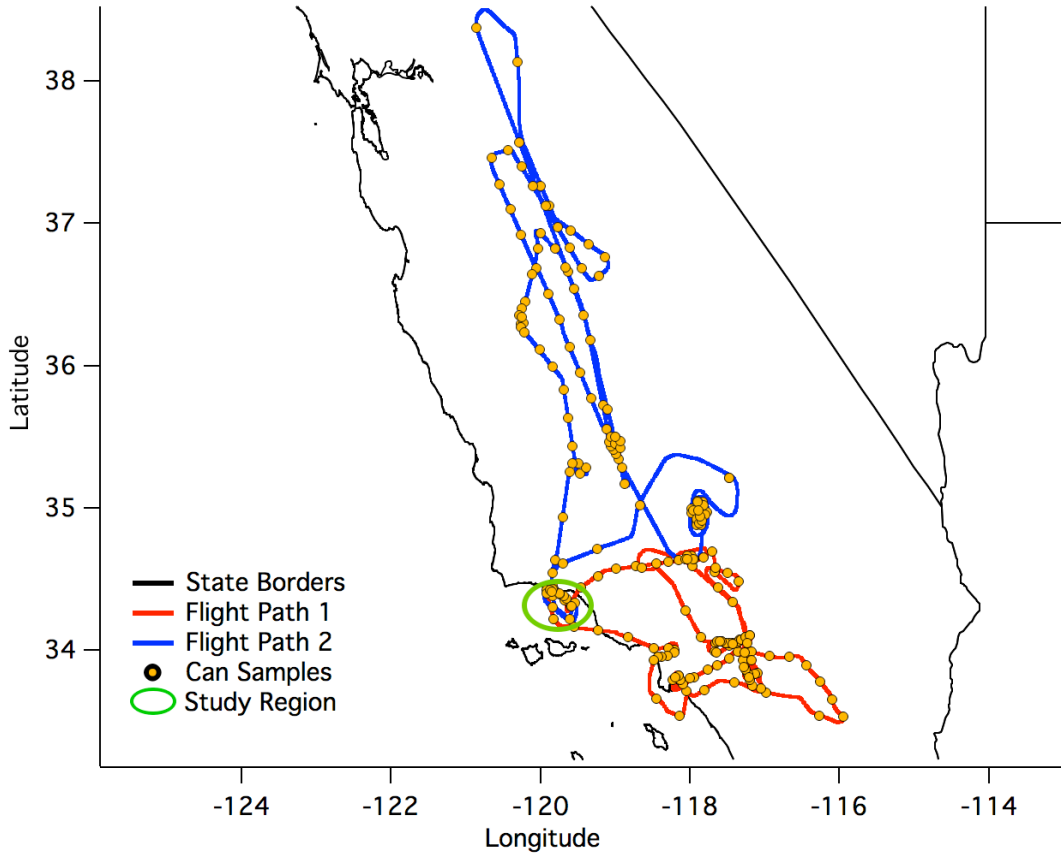

Figure 5. Sampling location of all the canisters collected during the research flights.

Five additional air samples were collected along the surface of the Santa Barbara Channel on June 21st, 2016. The canisters were filled from a height approximately 5 meters off the ocean surface on a small dive boat at various locations on the Santa Barbara Channel. The first sample was taken in a region with little kelp present to serve as a background concentration. The second and third canisters were taken over the Mohawk Kelp Forest and the Isla Vista Kelp Forest respectively. The fourth sample was collected roughly 80 meters from Platform Holly, an offshore oil well that is part of the Ellwood Oil Field. The final surface sample was taken at Coal Oil point on the periphery of an oil slick (Figure 6).

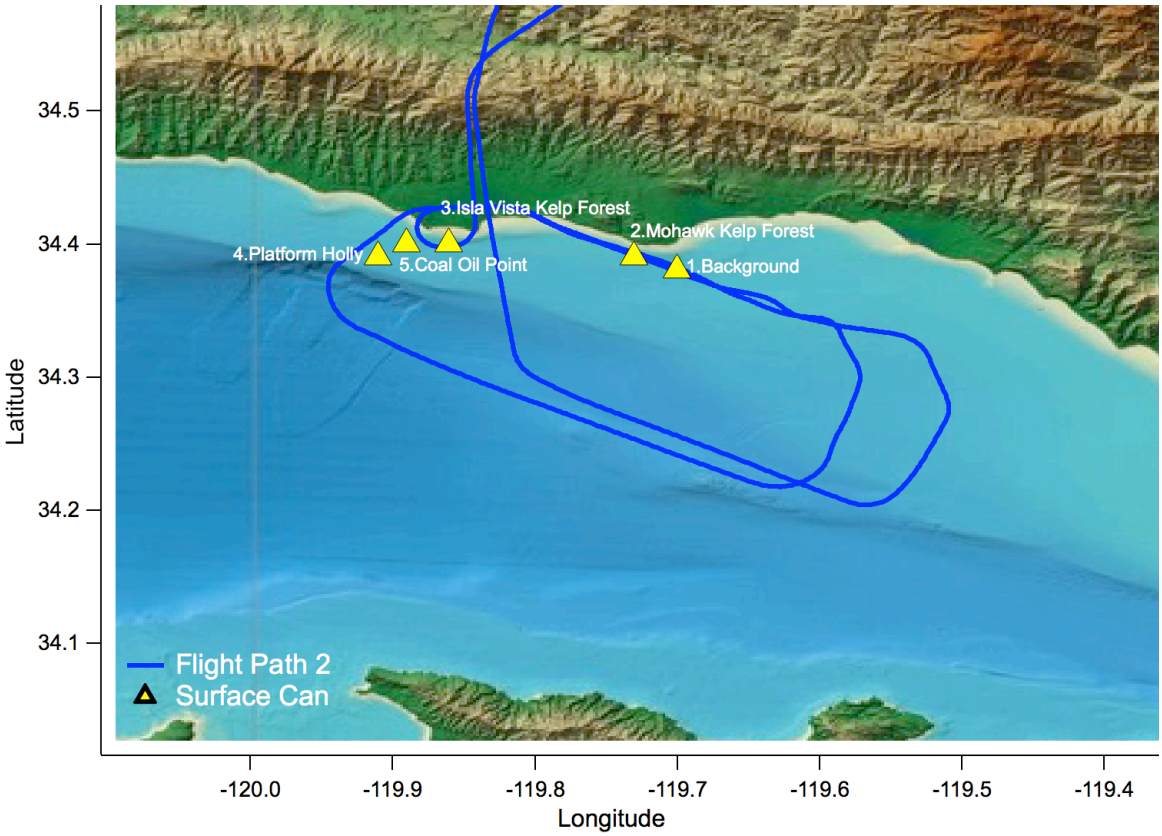

Figure 6. Surface can sampling sites in the Santa Barbara Channel on June 21st, 2016.

Sample Analysis

Canisters were analyzed in the Rowland-Blake laboratory at the University of California, Irvine (UCI) utilizing gas chromatography (GC) with flame ionization detection (FID), electron capture detection (ECD), and mass spectrometric detection (MSD). Each sample was analyzed for more than 100 selected trace gases, including C1-C10 nonmethane hydrocarbons (NMHCs), C1-C2 halocarbons, C1-C5 alkyl nitrates, and selected sulfur compounds. For more information regarding sample analysis, readers are referred to the Colman et al. (2001) and Simpson et al. (2010) publications.

Sample Grouping

After the lab analysis, the concentrations of sulfur-containing compounds, specifically OCS, DMS, CS_2, $CHBr_3$, and CH_3I were compared for twenty samples collected in the study region over the Santa Barbara Channel from aircraft and surface sampling (Figure 7). The vertical distribution of samples collected were used to categorize them into three groups. The first group was comprised of the five samples taken at the surface. The second group included four samples taken from 50-1,500 ft (15-460 m). The third group included eleven samples taken from 1,500-4,000 ft (460-1,250 m) (Figure 8). A vertical profile was analyzed to determine the boundary layer height for the day of sampling. The planetary boundary layer (PBL) is the lowest layer of the atmosphere that makes contact with the Earth's surface and is highly influenced by surface energy and moisture. It's height fluctuates due to radiative forcing (Dai et al., 2014), and this layer is generally homogenous so theoretically should have similar concentrations of given compounds throughout the PBL. With an approximated boundary layer height of 1,500 ft., these three distinct groups were chosen to produce a vertical

profile of the compounds from the surface, below the boundary layer, and above the boundary layer.

Data Analysis

To eliminate any samples potentially affected by the Sherpa fire (County of Santa Barbara, 2016), the samples were plotted against acetonitrile (CH_3CN) concentrations measured by the Proton-Transfer-Reaction Mass Spectrometer (PTR-MS) instrument onboard the DC-8. This instrument measures in-situ detection of gaseous volatile organic compounds (VOCs) at trace levels (pptv), and is designed to resist aircraft vibrations during boundary layer flights, take-off and landing (Wisthaler et al., 2013). Since acetonitrile and OCS are both indicators of biomass burning, any samples collected in regions of elevated acetonitrile were excluded from the analysis to isolate marine-sourced compounds (Figure 9). Two samples in the 50-1,500 ft (15-460 m) group were collected in regions with elevated acetonitrile and thus removed from the study.

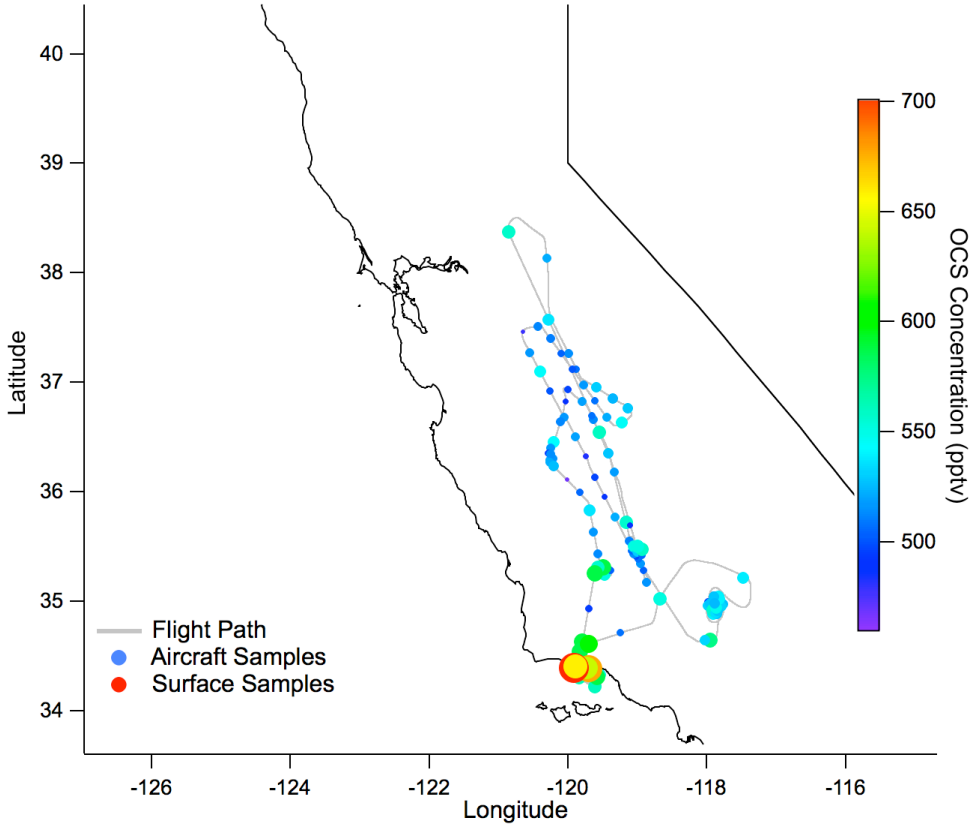

Figure 7. OCS concentration for each sample overlaying the second flight path. Sample diameter sized and colored by OCS concentration with high concentrations centered on Santa Barbara Channel.

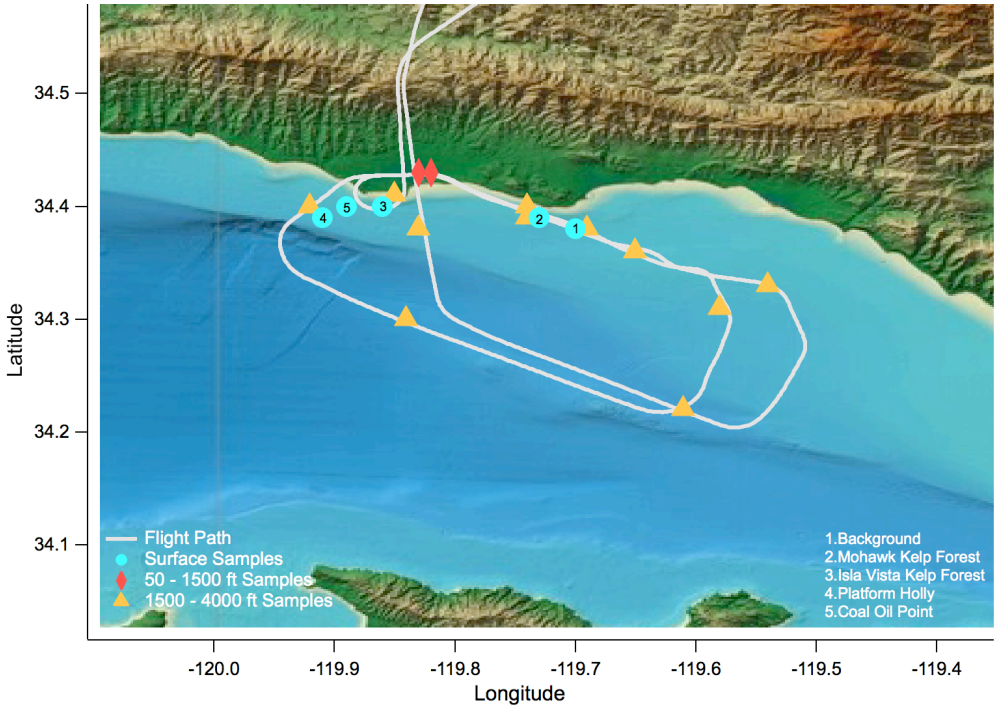

Figure 8. Three sample groups based on sampling altitude and plotted on flight path.

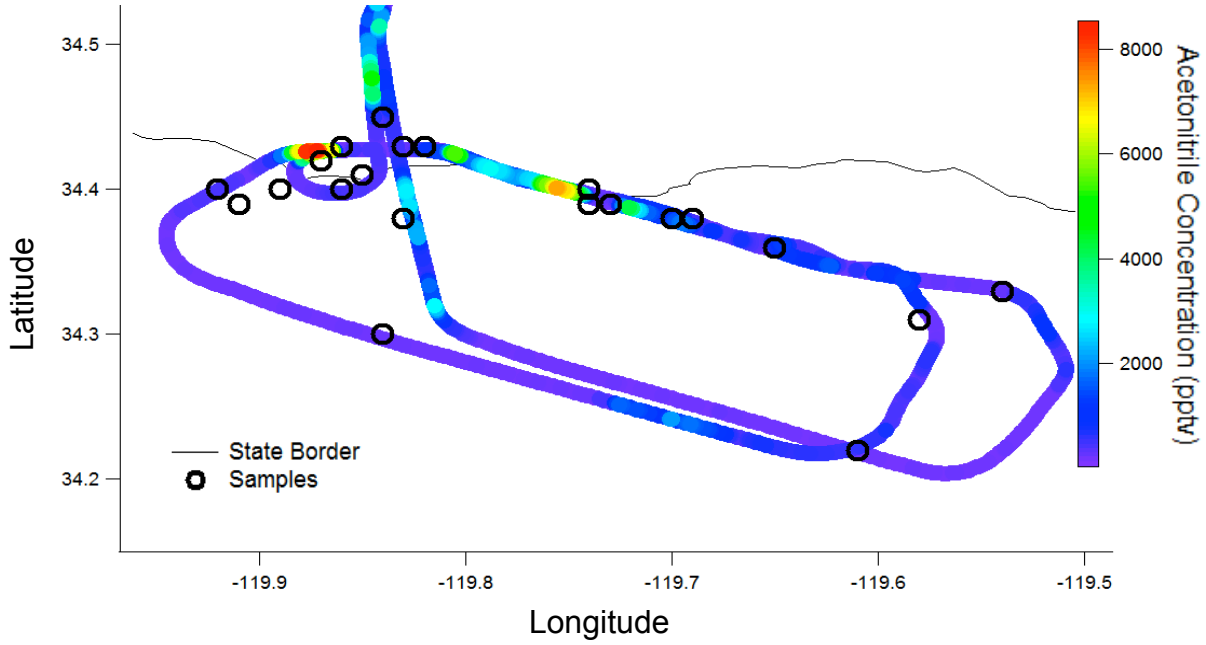

Figure 9. Samples plotted against acetonitrile concentrations measured by the PTR-MS instrument on June 18th, 2016.

The final step for processing the 2016 data was analyzing the concentrations of the higher altitude samples to calculate an average mixing ratio above the study region for OCS, DMS, and CS_2. A mixing ratio refers to the abundance of one constituent in a mixture relative to abundance of all other components (Jacobson, 2005). The concentrations of samples collected from altitudes near and above 1 km were averaged. These mixing ratios as shown in table 2 were then used as background concentrations to show any enhancements in the 2016 sample groups.

Table 2. Calculated mixing ratios using concentrations from samples collected at or above 1 km over the Santa Barbara Channel for OCS, DMS, and CS_2.

	Average Mixing Ratio, pptv (mean ± SE)
OCS	594 ± 31
DMS	1.3 ± 1.1
CS_2	2.2 ± 0.6

Comparison Between SARP Campaigns

Concentrations of OCS in the five surface samples from the 2016 SARP campaign were then compared to OCS concentrations from samples collected during previous SARP campaigns (2009-2015). Thirty five samples were taken during or near the same week of the year at various sites including Gaviota State Beach, El Capitan Beach, Haskell's Beach, UCSB, Monterey Bay, and several locations throughout the Santa Barbara Channel during the 2009, 2012, 2014, and 2015 SARP campaigns (Appendix, Table A1).

Sea Surface Temperature Data

Sea surface temperature (SST) has a major influence on the outgassing of marine tracers due to changes in biological productivity (Behrenfeld et al., 2006), therefore, SST data from the Santa Barbara Channel was obtained from the National Oceanic and Atmospheric Administration's (NOAA) National Data Buoy Center. Two buoy stations were selected from the Santa Barbara Basin to compare SST during the current and previous SARP campaigns (Appendix, Figure A1). Station ID 46054 is a 3-meter discus buoy that measures SST from 0.6 meters below the water line and is located 38 nautical miles west of Santa Barbara, CA. The second station, ID 46053 is a 2.3-meter discus buoy measuring SST from 1 meter below the water line and located 12 nautical miles southwest of Santa Barbara, CA (Figure 10). The SST data from these stations was obtained for the years of 1997-98, 2009, 2012, 2014-2016, and averaged for three months, May-August, to account for the time of year sampling occurs (Table 3). The years 1997-98 were chosen because of the high SST anomalies recorded by buoys during that year's record-breaking El Niño event (Hall et al, 2010). The years 2009, 2012, and 2014-2016

were chosen because of the presence of surface samples collected during these specified years' SARP campaigns.

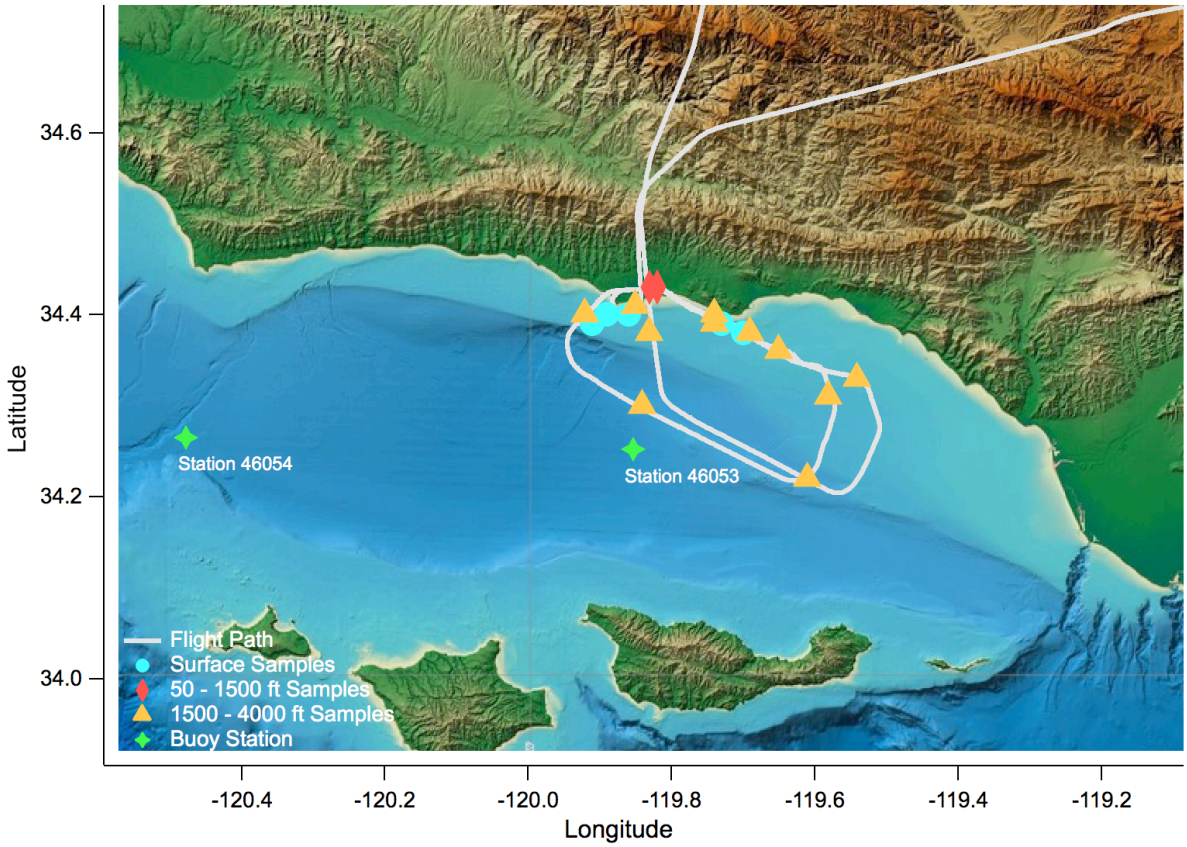

Figure 10. Final analysis samples and buoy stations plotted.

Operational SST Anomaly Charts from NOAA/NESDIS (National Environmental Satellite, Data and Information Service) for 1997-98, 2009, 2012, and 2014-2016 were obtained for data comparison with samples from the SARP campaigns (Appendix, Figures A2-A7). NOAA/NESDIS produce the SST anomaly by subtracting the long-term mean SST for a given location and the time of year from the current instrument reading. A positive anomaly value can be interpreted as a warmer than average SST whereas a negative anomaly means a cooler than average SST. SST anomalies are useful in assessing the development of ENSO events and were used to investigate potential effects

on marine tracers in collected samples.

Table 3. Hourly SST data extracted from NOAA's buoy stations located in the Santa Barbara Channel and averaged for three months, May 18th – August 18th of 1997-1998, 2009, 2012, 2014-2016. Buoy station IDs are 46054 and 46053.

Year	*Station ID 46054 SST, °C*	*Station ID 46054 SST, °C*
1997	15.59	no data
1998	15.24	16.90
2009	15.96	16.32
2012	13.88	15.83
2014	15.83	17.79
2015	15.61	17.49
2016	14.56	15.38

Statistical Analysis

The average concentration of OCS, DMS, and CS_2 were calculated for each sample group from the 2016 study region with a standard deviation and standard error. The standard deviation, σ, was calculated as shown in equation 4:

$$\sigma = \sqrt{\sum \frac{(x - x)^2}{(n-1)}} \qquad (1)$$

where *x* is the sample mean and *n* is the sample size. The standard error was calculated by dividing the standard deviation of the mean by the square root of n, the sample size.

A one-way analysis of variance (ANOVA) test was used to determine statistically significant differences between the means of surface samples from previous SARP campaigns and data collected in 2016. A Tukey's HSD (honestly significant difference) test was used to confirm where the differences detected by the ANOVA test occurred.

RESULTS

Whole air samples, 13 taken from the aircraft and 5 taken from the ocean's surface, were analyzed for sulfur-containing compounds including OCS, DMS, and CS_2. Other marine tracers such as $CHBr_3$ and CH_3I were also measured during the study and were also analyzed. Samples were divided into three groups based on sampling altitude: 0-50 ft (0-15 m, taken at the surface), 50-1,500 ft (15-460 m, taken from the aircraft within the boundary layer), and 1,500-4,000 ft (460-1,250 m, above the boundary layer). The 2016 samples were also compared to data from the 2009-2015 SARP campaigns collected near the 2016 study region and categorized using the same methods. Box and whisker plots were used to compare samples collected at varying altitudes. The boxes encompass the median, the upper quartile, and the lower quartile. The solid line in the box is the median, the upper edge of the box or 75^{th} quartile is where 25% of data is greater than that value, and the lower edge of the box or 25^{th} quartile is where 25% of data is less than that value. The two lines, or whiskers, represent the maximum and minimum values, points outside of this range are considered outliers. Lastly, SST data collected from two buoy stations in the Santa Barbara Channel was examined for any correlation between SST and elevated concentrations of sulfur-containing compounds.

Concentrations of Sulfur-Containing Compounds

Surface samples all exhibited elevated concentrations of OCS in comparison to samples taken from the aircraft, with an average of 666 ± 12 pptv and a maximum concentration of 706 pptv (Figures 11-12). The average concentration, 666 pptv was also greater than the calculated background concentration (Table 2) of 594 pptv.

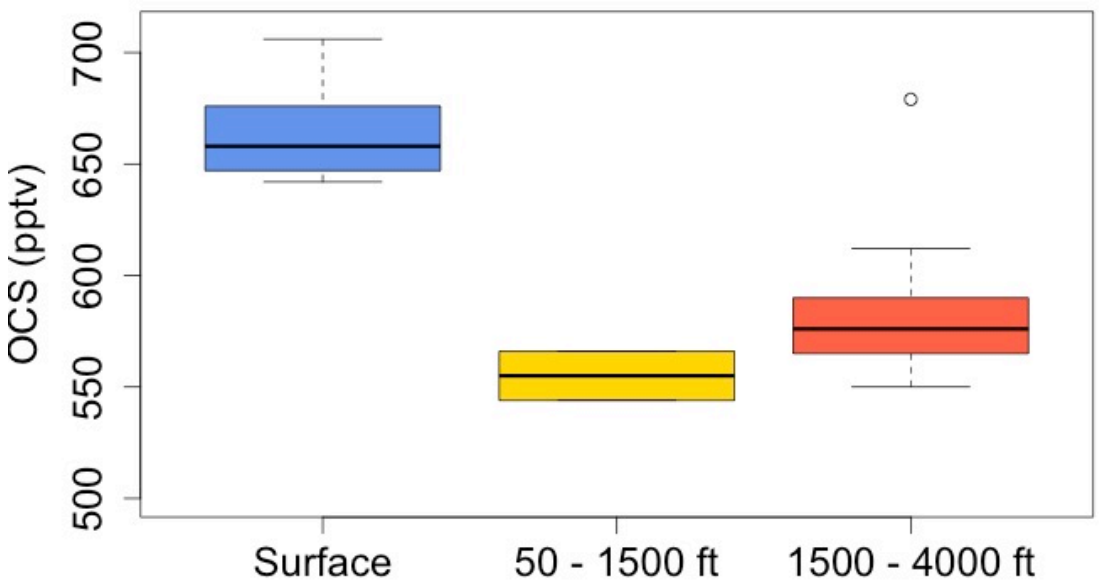

Figure 11. Box plot of the concentrations of OCS over the Santa Barbara Channel during the 2016 SARP campaign.

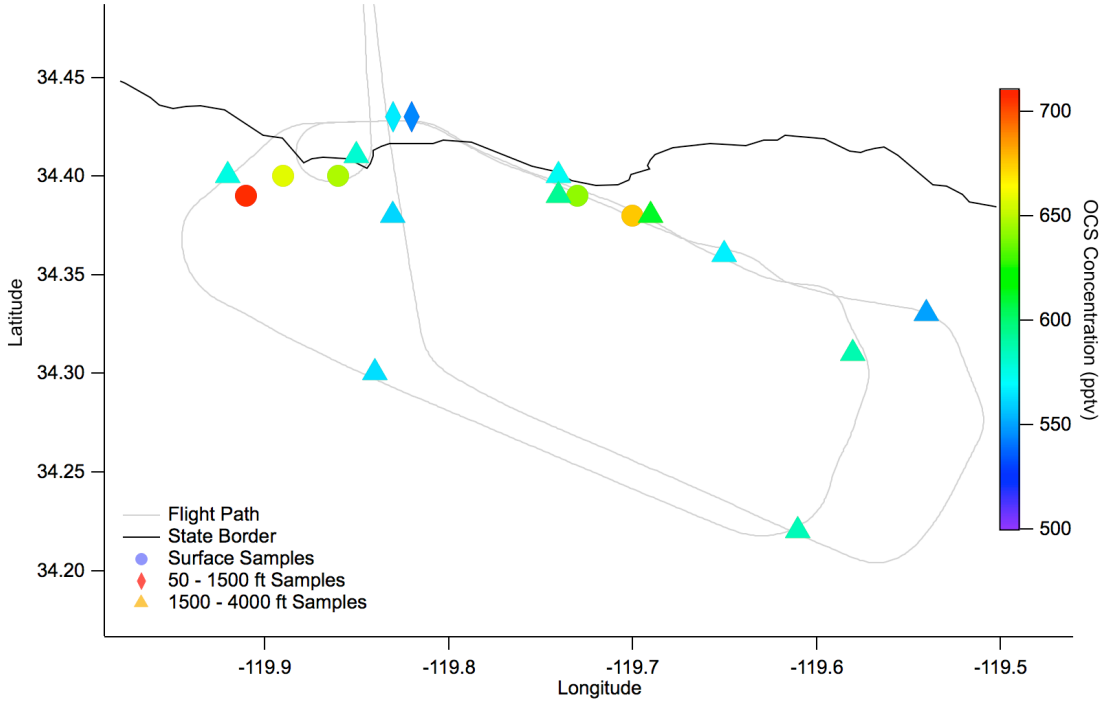

Figure 12. OCS concentrations for 2016 aircraft and surface samples with clear enhancements of OCS in the surface samples.

The average concentration of DMS in the surface samples was 34.7 ± 18.6 pptv (Figure 13). The surface sample concentration was about 38 times greater than the calculated mixing ratio of 1.3 ± 1.1 pptv (Table 2).

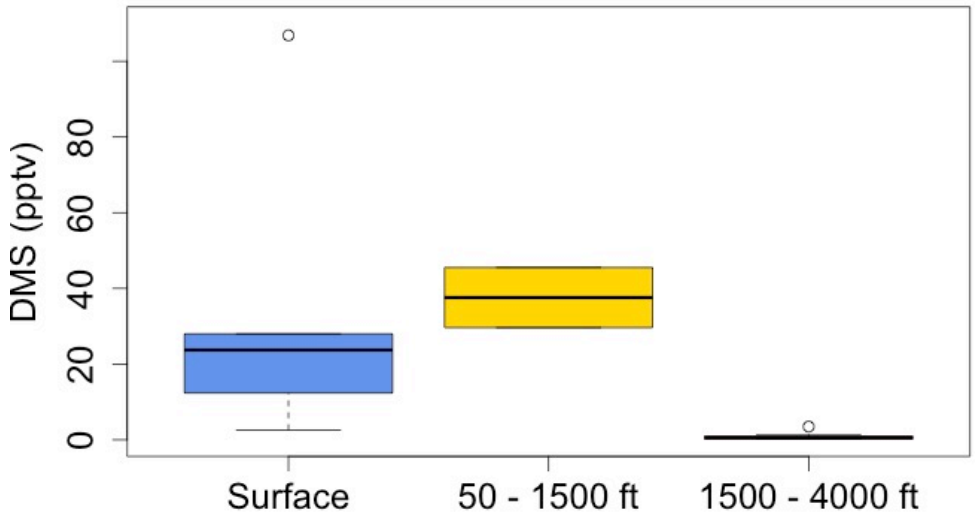

Figure 13. Box plot of the concentrations of dimethyl sulfide (DMS) over the Santa Barbara Channel during the 2016 SARP campaign.

The average concentration of CS_2 in the surface samples was found to be 2.84 ± 0.34 pptv (Figure 14). The surface concentrations were close in relation to the calculated mixing ratio of CS_2 which was 2.2 ± 0.6 (Table 2).

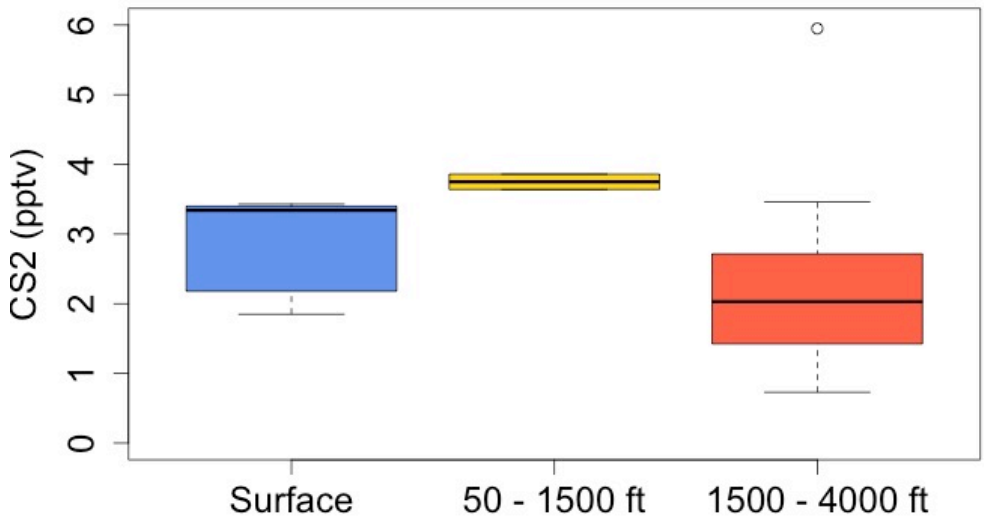

Figure 14. Box plot of the concentrations of carbon disulfide (CS_2) over the Santa Barbara Channel during the 2016 SARP campaign.

Concentrations of Marine Tracers

The compounds $CHBr_3$ and CH_3I were included in the analysis as examples of marine-sourced gases that had conventional trends of decreasing concentration with increasing altitude (Palmer, 2010). The box plots show typical profiles for a marine-sourced gas (Figures 15-16).

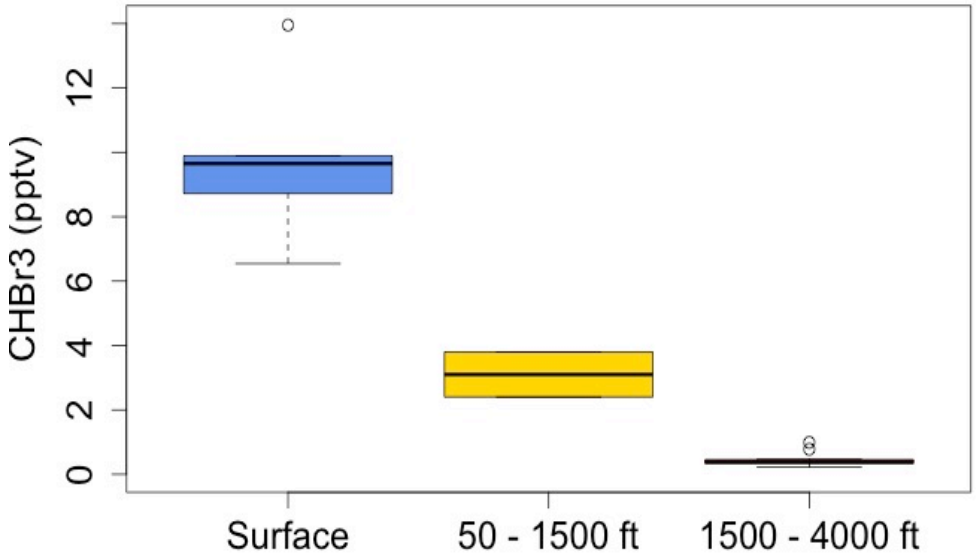

Figure 15. Box plot of the concentrations of bromoform ($CHBr_3$) over the Santa Barbara Channel during the 2016 SARP campaign.

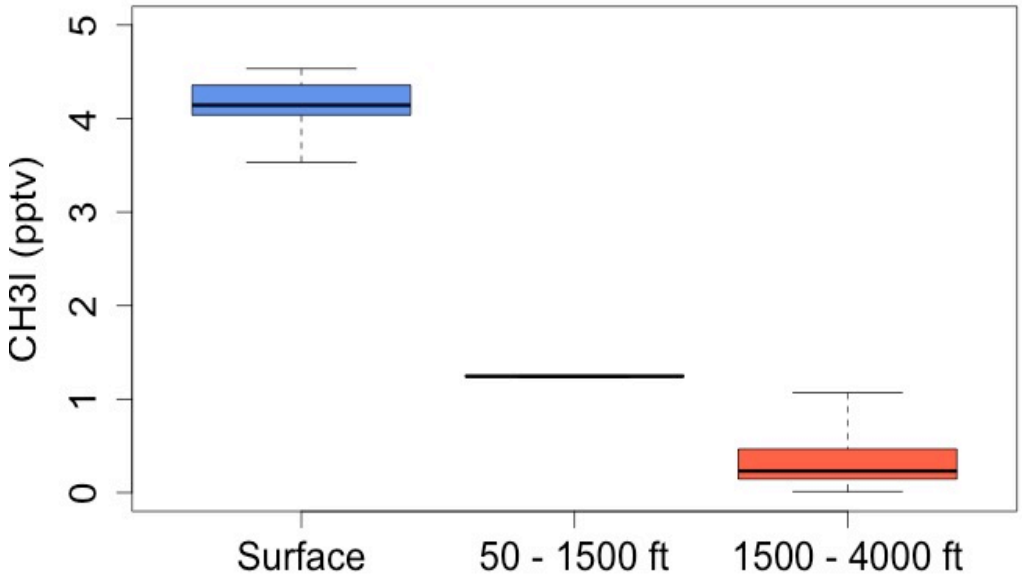

Figure 16. Box plot of the concentrations of methyl iodide (CH_3I) over the Santa Barbara Channel during the 2016 SARP campaign .

Comparison of Carbonyl Sulfide Concentrations from 2009-2016

The 2016 samples taken over the Santa Barbara Channel were compared to samples taken from previous SARP campaigns in the years 2009, 2012, 2014, and 2015. The average concentration for the 2016 surface cans was 666 ± 12 pptv, whereas the average concentration for the surface cans from 2009 was 555 ± 6 pptv, was 438 ± 5 for the year 2012, was 508 ± 6 in 2014, and was 548 ± 7 in 2015 (Figures 17-18). The combined average of the surface cans from previous SARP campaigns was 526 ± 8, which is substantially less than the surface concentration from 2016.

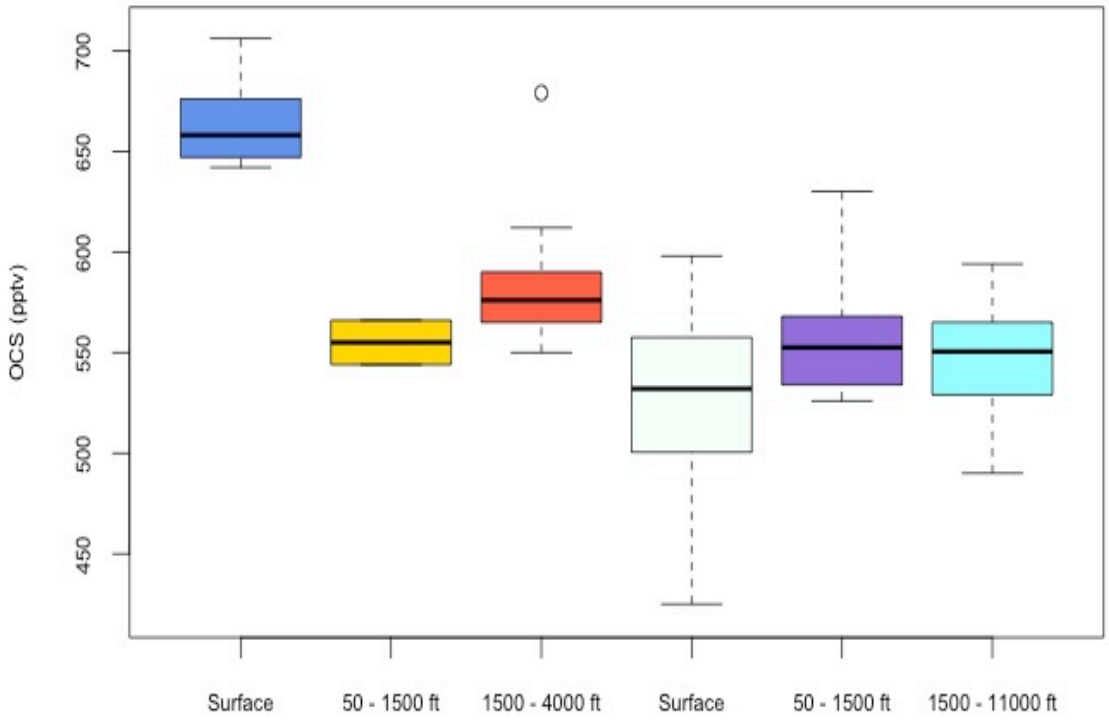

Figure 17. Box plot comparison of 2016 OCS concentrations (left) to 2009-2015 OCS concentrations (right) taken near or in the 2016 study region.

There was a statistically significant difference between the surface sample groups taken in 2009, 2012, and 2014-2016 as determined by a one-way ANOVA ($F(4,35)=69.09$, $p<0.0001$). Post-hoc Tukey's HSD tests showed that the significant

differences detected by the ANOVA occurred between all the sample groups ($p<0.01$) except for the comparison of 2015 to 2009 which was insignificant.

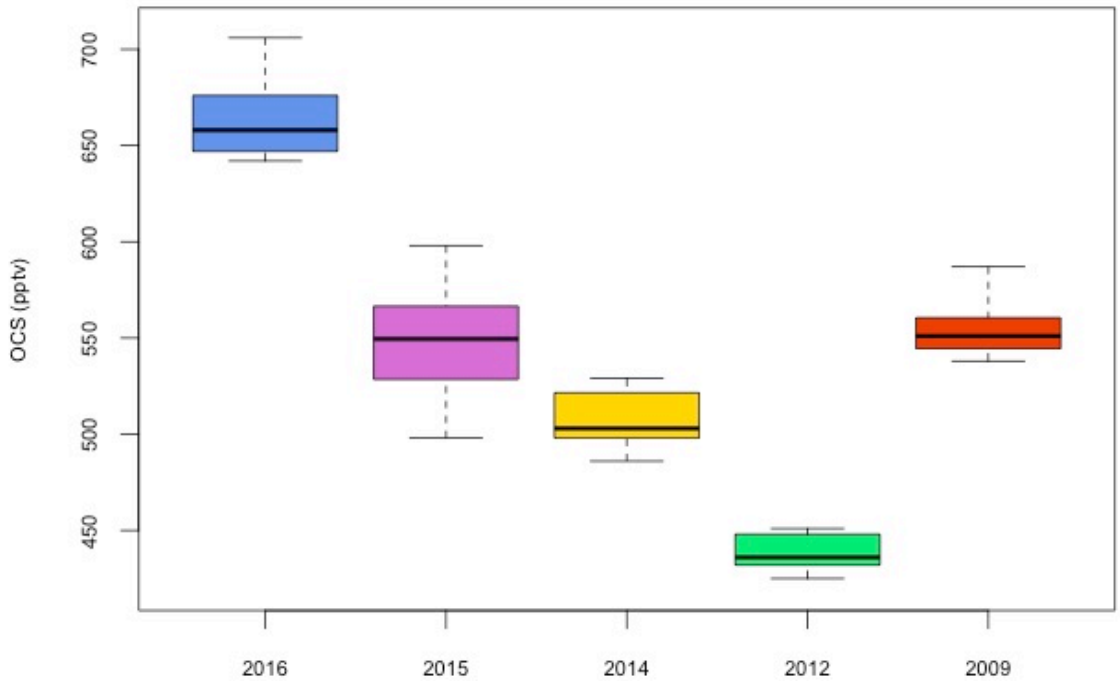

Figure 18. Box plot comparison of OCS concentrations in surface samples taken from 2009, 2012, and 2014-2016.

DISCUSSION

The concentrations of OCS, DMS, CS_2, $CHBr_3$, and CH_3I were analyzed in the samples collected during the 2016 SARP campaign. It was expected that these compounds would have higher concentrations over the Santa Barbara Channel since they are all marine-influenced or sourced. Conventional vertical distribution was anticipated, with a mixed boundary layer and homogenous distribution in the free troposphere. However, OCS showed greater concentrations at the surface which was unexpected considering analysis of data from previous years. The relatively long atmospheric lifetime of OCS (2-7 years) would lead to a more homogenous boundary layer, therefore, previous campaigns showed samples collected aboard the DC-8 in the boundary layer to be relatively similar to samples collected at the sea surface (Xu et al., 2001). The surface samples showed enhancements in OCS concentration compared to samples collected aboard the aircraft, with nearly all the samples having a concentration higher than 650 pptv (Figure 12), indicating a unique phenomenon captured during 2016.

Due to the short atmospheric lifetime of DMS of about 12 to 48 hours (Keller et al., 1989; Brühl et al., 2012), it should not be present at altitudes higher than the second sample group (50-1,500 ft). The samples showed a conventional trend of dilution with increasing altitude for DMS concentration (Figure 13). We also expected CS_2 to follow a conventional trend of decreasing concentration with increasing altitude. The samples did show this trend of dilution, with greater variance than the DMS concentrations (Figure 14). CS_2 has an atmospheric lifetime of 7-12 days (Khalil & Rasmussen, 1984; Brühl et al., 2015) which is slightly longer than that of DMS, and which may explain the variability in the sample groups taken above the surface.

We expected that $CHBr_3$ and CH_3I would exhibit conventional trends (Palmer, 2010) and show dilution with increasing altitude, as was shown by the data. These compounds, both of which have an atmospheric lifetime of about 1-4 weeks (Stemmler et al., 2013; Stemmler et al., 2014), were included to illustrate a traditional vertical profile of a marine-influenced compound and its concentration as altitude increases (Figures 15-16).

The final box plot comparisons were between the 2016 SARP campaign and previous SARP campaigns. In Figure 17, the gradient of OCS concentrations in the 2016 samples is plotted next to the OCS concentrations from combined data during the 2009, 2012, 2014, and 2015 campaigns. With hundreds of samples collected during SARP campaigns and thousands of samples processed by the Rowland-Blake Laboratory in UCI, the OCS gradient evident from the 2016 SARP campaign is showing a unique phenomenon at work. Elevated levels of OCS have never been seen from the plane before this year (Figure 18), indicating that OCS emissions must be measured using surface samples if estimates from the ocean and accurate profiles are to be evaluated. Without surface samples from this year and relying only on aircraft samples, this elevated OCS phenomenon would have been missed.

In an attempt to explain this OCS surface phenomenon, SST data was collected from two buoy stations located in the Santa Barbara Channel to determine whether changes in SST could have caused an increase in OCS production and thus outgassing into the atmosphere. The buoy data coupled with SST anomaly maps sourced from NOAA/NESDIS (Appendix, Figures 2-7) indicate that there was a slight increase in the surface water temperature for the 2015-2016 year, but that the SST at the time of

sampling in June was beginning to fall below average (negative anomalies). Previous years had variance in SST with some small temperature increases occurring (positive anomalies). Behrenfeld et al. (2006) describes how fluctuations in temperature are connected to the productivity of phytoplankton in the world's oceans. For much of the ocean, warmer surface temperatures correspond to lower oceanic biomass and productivity (Doney, 2006). Phytoplankton growth depends on temperature, nutrient, and light availability, with most of the necessary nutrients being supplied to the surface waters from the mixing and upwelling of cold, nutrient-rich deep water (Doney, 2006). The highest levels of phytoplankton biomass are found along the Equator, in temperature and polar latitudes, and near the western boundaries of continents (Doney, 2006). As shown by Behrenfeld et al. (2006), the increase in phytoplankton in 1997-98 matched the cold tongue phase of the El Niño event that year, implicating that increases in productivity occur with decreases in SST. Therefore, the SST data from the years 2015-16 may have matched the events of the most recent ENSO event and caused a slight increase in phytoplankton productivity, thus increasing ocean outgassing. However, the SST data do not strongly correlate with OCS surface concentrations (R^2=0.1028), requiring further investigation to determine the cause of the 2016 enhancements.

Ocean-surface OCS concentrations were found to highly correlate with surface water primary productivity (Andreae & Ferek, 1992), therefore warm waters induced by El Niño could have an effect on OCS concentrations. Buoy and SST anomaly data were also collected for the years 1997-1998 because of the historical El Niño event occurring during this time, and with the intent of comparing them to the 2015-2016 SST data that marked another historical El Niño event. The 2015-2016 buoy data do have generally

higher SST values than the temperatures in 1997-1998 (Table 3), but we lack OCS concentration data from 1997-1998 to permit correlation between El Niño events and OCS concentrations.

In summary, elevated OCS concentrations were detected at the surface from samples over the Santa Barbara Channel taken in June, 2016. These results are a big deal because they are implying that aircraft measurements are underestimating emissions of compounds like OCS at the surface, since aircraft sampling typically occurs at a minimum altitude of 500 ft which is not low enough to capture surface elevations. This underestimation has huge influences on global models and accurate estimates of emission sources. Recognizing the limitation of this year's data set with only five surface samples, future work for this study should start with collecting more surface samples from the Santa Barbara Channel to further track the OCS surface phenomenon from this year. It is important to continue measuring OCS to both strengthen our understanding of its sources and sinks, and to better understand its implications for countering global climate change through its contribution to stratospheric aerosols (Brühl et al., 2012), which exert a radiative cooling force and act to offset the effects of global warming.

ACKNOWLEDGEMENTS

This study was supported and made possible by the National Aeronautics and Space Administration 2016 Student Airborne Research Program (NASA SARP) and the National Suborbital Education and Research Center (NSERC). Special thanks to the NASA SARP program coordinator and project manager, Dr. Emily Schaller, the Associate Director for Research of the NASA Earth Science Division (ESD), Dr. Jack Kaye, the NASA Armstrong Flight Research Center, the 2016 DC-8 flight crew, the Rowland-Blake lab at the University of California, Irvine, and my fellow 2016 NASA SARP interns.

I would like to extend gratitude to my mentors during SARP 2016, Dr. Don Blake and Stacey Hughes of University of California, Irvine, who gave continual guidance and support throughout my project and acted as readers of this thesis.

An additional thank you to Professor Colin Robins for his generous service as a reader of this thesis, for recommending me for the NASA SARP program, and for his guidance and encouragement in the years preceding this project.

REFERENCES

Andreae, M.O. and Ferek, R.J. (1992). Photochemical production of carbonyl sulfide in seawater and its emission to the atmosphere. *Global Biogeochemical Cycles,* 6, 175-183. https://doi.org/10.1029/91GB02809

Arsene, C., Barnes, I., & Becker, K. H. (1999). FT-IR product study of the photo-oxidation of dimethyl sulfide: Temperature and O2 partial pressure dependence, *1*(24), 5463–5470. https://doi.org/10.1039/A907211J

Bandy, A. R., Thornton, D. C., Scott, D. L., Lalevic, M., Lewin, E. E., & Driedger, A. R. (1992). A time series for carbonyl sulfide in the northern hemisphere. *Journal of Atmospheric Chemistry*, *14*(1–4), 527–534. https://doi.org/10.1007/BF00115256

Barnes, I., Becker, K. H., & Patroescu, I. (1994). The tropospheric oxidation of dimethyl sulfide: A new source of carbonyl sulfide. *Geophysical Research Letters*, *21*(22), 2389–2392. https://doi.org/10.1029/94GL02499

Barnes, I., Becker, K. H., & Patroescu, I. (1996). FTIR product study of the OH initiated oxidation of dimethyl sulphide: Observation of carbonyl sulphide and dimethyl sulphoxide. *Atmospheric Environment*, *30*(10–11), 1805–1814.

Bates, T. S., Lamb, B. K., Guenther, A., Dignon, J., & Stoiber, R. E. (1992). Sulfur emissions to the atmosphere from natural sourees. *Journal of Atmospheric Chemistry*, *14*(1–4), 315–337. https://doi.org/10.1007/BF00115242

Behrenfeld, M. J., O'Malley, R. T., Siegel, D. A., McClain, C. R., Sarmiento, J. L., Feldman, G. C., … Boss, E. S. (2006). Climate-driven trends in contemporary ocean productivity. *Nature*, *444*(7120), 752–755. https://doi.org/10.1038/nature05317

Blake, N. J., Campbell, J. E., Vay, S. A., Fuelberg, H. E., Huey, L. G., Sachse, G., … Blake, D. R. (2008). Carbonyl sulfide (OCS): Large-scale distributions over North America during INTEX-NA and relationship to CO2. *Journal of Geophysical Research: Atmospheres*, *113*(D9), D09S90. https://doi.org/10.1029/2007JD009163

Blake, N. J., Streets, D. G., Woo, J.-H., Simpson, I. J., Green, J., Meinardi, S., … Blake, D. R. (2004). Carbonyl sulfide and carbon disulfide: Large-scale distributions over the western Pacific and emissions from Asia during TRACE-P. *Journal of Geophysical Research: Atmospheres*, *109*(D15), D15S05. https://doi.org/10.1029/2003JD004259

Blomquist, B. W., Bandy, A. R., Thornton, D. C., & Chen, S. (1993). Grab sampling for the determination of sulfur dioxide and dimethyl sulfide in air by isotope dilution gas chromatography/mass spectrometry. *Journal of Atmospheric Chemistry*, *16*(1), 23–30. https://doi.org/10.1007/BF00696621

Brühl, C., Lelieveld, J., Crutzen, P. J., & Tost, H. (2012). The role of carbonyl sulphide as a source of stratospheric sulphate aerosol and its impact on climate. *Atmos. Chem. Phys.*, *12*(3), 1239–1253. https://doi.org/10.5194/acp-12-1239-2012

Brühl, C., Lelieveld, J., Tost, H., Höpfner, M., & Glatthor, N. (2015). Stratospheric sulfur and its implications for radiative forcing simulated by the chemistry climate model EMAC. *Journal of Geophysical Research. Atmospheres*, *120*(5), 2103–2118. https://doi.org/10.1002/2014JD022430

Calvert, J. G., Orlando, J. J., Stockwell, W. R., & Wallington, T. J. (2015). *The Mechanisms of Reactions Influencing Atmospheric Ozone*. Oxford University Press.

Carroll, M. A., Heidt, L. E., Cicerone, R. J., & Prinn, R. G. (1986). OCS, H2S, and CS2 fluxes from a salt water marsh. *Journal of Atmospheric Chemistry*, *4*(3), 375–395. https://doi.org/10.1007/BF00053811

Charlson, R. J., J. Langner, and H. Rodhe (1990), Sulfate aerosol and climate, Nature, 348(22), doi:10.1038/348022a0.

Chin, M., & Davis, D. D. (1995). A reanalysis of carbonyl sulfide as a source of stratospheric background sulfur aerosol. *Journal of Geophysical Research*, *100*(D5), 8993. https://doi.org/10.1029/95JD00275

Coffey, M. T., & Hannigan, J. W. (2010). The temporal trend of stratospheric carbonyl sulfide. *Journal of Atmospheric Chemistry*, *67*(1), 61. https://doi.org/10.1007/s10874-011-9203-4

Colman, J. J., Swanson, A. L., Meinardi, S., Sive, B. C., Blake, D. R., & Rowland, F. S. (2001). Description of the Analysis of a Wide Range of Volatile Organic Compounds in Whole Air Samples Collected during PEM-Tropics A and B. *Analytical Chemistry*, *73*(15), 3723–3731. https://doi.org/10.1021/ac010027g

Commane, R., Herndon, S. C., Zahniser, M. S., Lerner, B. M., Mcmanus, J. B., Munger, J. W., Nelson, D. D., & Wofsy, S. C. (2013). Carbonyl sulfide in the planetary boundary layer: Coastal and continental influences. *Journal of Geophysical Research: Atmospheres, 118*(14). doi:10.1002/jgrd.50581

Commane, R., Meredith, L. K., Baker, I. T., Berry, J. A., Munger, J. W., Montzka, S. A., … Wofsy, S. C. (2015). Seasonal fluxes of carbonyl sulfide in a midlatitude forest. *Proceedings of the National Academy of Sciences*, *112*(46), 14162–14167. https://doi.org/10.1073/pnas.1504131112

County of Santa Barbara. (2016). Sherpa Fire Information and Updates. Retrieved from https://countyofsb.org/sherpa-fire.sbc

Crutzen, P. J. (1976), The possible importance of OCS for the sulfate layer of the stratosphere. *Geophysical Research Letter, 3*(2), 73 – 76. doi:10.1029/GL003i002p00073.

Cutter, G. A., Cutter, L. S., & Filippino, K. C. (2004). Sources and cycling of carbonyl sulfide in the Sargasso Sea. *Limnology and Oceanography, 2*. doi:10.4319/lo.2004.49.2.0555.

Dai, C., Wang, Q., Kalogiros, J. A., Lenschow, D. H., Gao, Z., & Zhou, M. (2014). Determining Boundary-Layer Height from Aircraft Measurements. *Boundary Layer Meteorology*, *152*(3), 277–302. https://doi.org/10.1007/s10546-014-9929-z

de Gouw, J. A., Warneke, C., Parrish, D. D., Holloway, J. S., Trainer, M., & Fehsenfeld, F. C. (2003). Emission sources and ocean uptake of acetonitrile (CH3CN) in the atmosphere. *Journal of Geophysical Research: Atmospheres*, *108*(D11), 4329. https://doi.org/10.1029/2002JD002897

Doney, S. C. (2006). Oceanography: Plankton in a warmer world. *Nature*, *444*(7120), 695–696. https://doi.org/10.1038/444695a

Ferm, R. J. (1957). The Chemistry Of Carbonyl Sulfide. *Chemical Reviews*, *57*(4), 621–640. https://doi.org/10.1021/cr50016a002

Finlayson-Pitts, B. J., & Pitts, J. N. (2000). *Chemistry of the upper and lower atmosphere: Theory, experiments, and applications*. San Diego: Academic Press.

Forster, P., Ramaswamy, V., Artaxo, P., Berntsen, T., Betts, R., Fahey, D.W., …Van Dorland, R. (2007). Changes in Atmospheric Constituents and in Radiative Forcing. *In: Climate Change 2007: The Physical Science Basis. Contribution of Working Group I to the Fourth Assessment Report of the Intergovernmental Panel on Climate Change* [Solomon, S., D. Qin, M. Manning, Z. Chen, M. Marquis, K.B. Avery, M.Tignor and H.L. Miller (eds.)]. Cambridge University Press, Cambridge, United Kingdom and New York, NY, USA.

Glatthor, N., Höpfner, M., Baker, I. T., Berry, J., Campbell, J. E., Kawa, S. R., … Clarmann, T. (2015). Tropical sources and sinks of carbonyl sulfide observed from space. *Geophysical Research Letters*, *42*(22), 10,082-10,090.

Hall, S. E., Bramer, D., Wojtowicz, D., Wilhelmson, B., & Ramamurthy, M. (2010). 1997 1998 El Niño. Retrieved September 30, 2014, from http://ww2010.atmos.uiuc.edu/(Gh)/guides/mtr/eln/rcnt.rxml

Jacobson, M. Z. (1999). *Fundamentals of atmospheric modeling*. Cambridge, UK: Cambridge University Press.

Jodwalis, C. M., Benner, R. L., & Eslinger, D. L. (2000). Modeling of dimethyl sulfide ocean mixing, biological production, and sea-to-air flux for high latitudes. *Journal of Geophysical Research: Atmospheres*, *105*(D11), 14387–14399. https://doi.org/10.1029/2000JD900023

Keller, M. D., Bellows, W. K., & Guillard, R. R. L. (1989). Dimethyl Sulfide Production in Marine Phytoplankton. In *Biogenic Sulfur in the Environment* (Vol. 393, pp. 167–182). American Chemical Society. Retrieved from http://dx.doi.org/10.1021/bk-1989-0393.ch011

Kettle, A. J. (2002), Global budget of atmospheric carbonyl sulfide: Temporal and spatial variations of the dominant sources and sinks, *Journal of Geophysical Research: Atmospheres*, 107(D22), 4658, doi:10.1029/2002JD002187.

Khalil, M. A. K., & Rasmussen, R. A. (1984). Global sources, lifetimes and mass balances of carbonyl sulfide (OCS) and carbon disulfide (CS2) in the earth's atmosphere. *Atmospheric Environment (1967)*, *18*(9), 1805–1813. https://doi.org/10.1016/0004 6981(84)90356-1

Kim, K.-H., & Andreae, M. O. (1987). Carbon disulfide in seawater and the marine atmosphere over the North Atlantic. *Journal of Geophysical Research: Atmospheres*, *92*(D12), 14733–14738. https://doi.org/10.1029/JD092iD12p14733

Kremser, S., Jones, N. B., Palm, M., Lejeune, B., Wang, Y., Smale, D., & Deutscher, N. M. (2015). Positive trends in Southern Hemisphere carbonyl sulfide. *Geophysical Research Letters*, *42*(21), 9473–9480.

Launois, T., Belviso, S., Bopp, L., Fichot, C. G., & Peylin, P. (2015). A new model for the global biogeochemical cycle of carbonyl sulfide - Part 1: Assessment of direct marine emissions with an oceanic general circulation and biogeochemistry model. *Atmospheric Chemistry and Physics*, *15*, 2295-2312. doi:10.5194/acp-15-2295 2015

Logan, J. A., McElroy, M. B., Wofsy, S. C., & Prather, M. J. (1979). Oxidation of CS2 and COS: sources for atmospheric SO2. *Nature*, *281*(5728), 185–188. https://doi.org/10.1038/281185a0

McPhaden, M. J. (1999). Genesis and Evolution of the 1997-98 El Niño. *Science*, *283*(5404), 950–954. https://doi.org/10.1126/science.283.5404.950

Mihalopoulos, N., Nguyen, B. C., Putaud, J. P., & Belviso, S. (1992). The oceanic source of carbonyl sulfide (COS). *Atmospheric Environment. Part A. General Topics*, *26*(8), 1383–1394. https://doi.org/10.1016/0960-1686(92)90123-3

Mihalopoulos, N., Putaud, J. P., Nguyen, B. C., & Belviso, S. (1991). Annual variation of atmospheric carbonyl sulfide in the marine atmosphere in the Southern Indian Ocean. *Journal of Atmospheric Chemistry*, *13*(1), 73–82. https://doi.org/10.1007/BF00048101

Miller, S. D., Marandino, C., & Saltzman, E. S. (2010). Ship-based measurement of air-sea CO2 exchange by eddy covariance. *Journal of Geophysical Research: Atmospheres*, *115*(D2), D02304. https://doi.org/10.1029/2009JD012193

Miller, S., Marandino, C., de Bruyn, W., & Saltzman, E. S. (2009). Air-sea gas exchange of CO2 and DMS in the North Atlantic by eddy covariance. *Geophysical Research Letters*, *36*(15), L15816. https://doi.org/10.1029/2009GL038907

Müller, M., Mikoviny, T., Haidacher, S., Hanel, G., Hartungen, E., Jordan, A., … Wisthaler, A. (2014). Development and deployment of a compact PTR-ToF-MS for Suborbital Research on the Earth's Atmospheric Composition (Vol. 16, p. 9809). Presented at the EGU General Assembly Conference Abstracts. Retrieved from http://adsabs.harvard.edu/abs/2014EGUGA..16.9809M

Moore, R. M., & Groszko,W. (1999). Methyl iodide distribution in the ocean and fluxes to the atmosphere. *Journal of Geophysical Research*, 104(C5), 11163-1171.

NOAA. (2016). NOAA Marine Environmental Buoy Database. Retrieved October, 2016, from http://www.nodc.noaa.gov/BUOY/

NOAA. (2016). Operational SST Anomaly Charts for 2016. Retrieved September, 2016, from http://www.ospo.noaa.gov/Products/ocean/sst/anomaly/

NOAA. (2016). Station 46054 Historical Data. Retrieved November, 2016 from http://www.ndbc.noaa.gov/station_history.php?station=46054

NOAA. (2016). Station 46053 Historical Data. Retrieved November, 2016 from http://www.ndbc.noaa.gov/station_page.php?station=46053

OCS, stratospheric aerosols and climate. (n.d.). Retrieved from http://www.nature.com/nature/journal/v283/n5744/pdf/283283a0.pdf

Palmer, C. J. (2010). Contrasting the surface ocean distribution of bromoform and methyl iodide; implications for boundary layer physics, chemistry and climate. *IOP Conference Series: Earth and Environmental Science*, *13*(1), 12004. https://doi.org/10.1088/1755-1315/13/1/012004

Perkins, L. (2016). El Niño: GMAO Daily Sea Surface Temperature Anomaly from 1997/1998 and 2015/2016. Retrieved September 30, 2016, from https://svs.gsfc.nasa.gov/4433

Saltzman, E. S., & Cooper, D. J. (1988). Shipboard measurements of atmospheric dimethylsulfide and hydrogen sulfide in the Caribbean and Gulf of Mexico. *Journal of Atmospheric Chemistry*, *7*(2), 191–209. https://doi.org/10.1007/BF00048046

Simpson, I. J., Colman, J. J., Swanson, A. L., Bandy, A. R., Thornton, D. C., Blake, D. R., & Rowland, F. S. (2001). Aircraft Measurements of Dimethyl Sulfide (DMS) Using a Whole Air Sampling Technique. *Journal of Atmospheric Chemistry*, *39*(2), 191–213. https://doi.org/10.1023/A:1010608529779

Simpson, I. J., Blake, N. J., Barletta, B., Diskin, G. S., Fuelberg, H. E., Gorham, K., …Blake, D. R. (2010). Characterization of trace gases measured over Alberta oil sands mining operations: 76 speciated C_2-C_{10} volatile organic compounds (VOCs), CO_2, CH_4, CO, NO, NO_2, NO_y, O_3 and SO_2. *Atmospheric Chemistry and Physics*, *10*(23), 11931 11954. doi:10.5194/acp-10-11931-2010.

Smythe-Wright, D., Boswell, S. M., Breithaupt, P., Davidson, R. D., Dimmer, C. H., & Diaz, L. B. (2006). Methyl iodide production in the ocean: Implications for climate change. *Global Biogeochemical Cycles, 20*(3). doi:10.1029/2005gb002642

Stemmler, I., Hense, I., & Quack, B. (2015). Marine sources of bromoform in the global open ocean – global patterns and emissions. *Biogeosciences*, *12*(6), 1967–1981. https://doi.org/10.5194/bg-12-1967-2015

Stemmler, I., Hense, I., Quack, B., & Maier-Reimer, E. (2013). Methyl iodide production in the open ocean. *Biogeosciences Discussions, 10*(11), 17549-17595. doi:10.5194/bgd-10-17549-2013

Sturges, W. T., Penkett, S. A., Barnola, J., Chappellaz, J., Atlas, E., & Stroud, V. (2001). A long-term record of carbonyl sulfide (COS) in two hemispheres from firn air measurements. *Geophysical Research Letters, 28*(21), 4095-4098. doi:10.1029/2001gl013958

Svoronos, P. D. N., & Bruno, T. J. (2002). Carbonyl sulfide: A review of its chemistry and properties. *Industrial and Engineering Chemistry Research, 41*(22), 5321 5336. doi:10.1021/ie020365n

Sze, N. D., & K.W. Ko, M. (1980). Photochemistry of COS, CS2, CH3SCH3 and H2S: Implications for the atmospheric sulfur cycle. *Atmospheric Environment (1967)*, *14*(11), 1223–1239. https://doi.org/10.1016/0004-6981(80)90225-5

Turner, S. M., & Liss, P. S. (1985). Measurements of various sulphur gases in a coastal marine environment. *Journal of Atmospheric Chemistry*, *2*(3), 223–232. https://doi.org/10.1007/BF00051074

Ulshöfer, V. S., & Andreae, M. O. (1997). Carbonyl Sulfide (COS) in the Surface Ocean and the Atmospheric COS Budget. *Aquatic Geochemistry*, *3*(4), 283–303. https://doi.org/10.1023/A:1009668400667

Warneck, P. (1988). *Chemistry of the natural atmosphere*. San Diego: Academic Press. Retrieved from Table of contents http://www.gbv.de/dms/bowker/toc/9780127356303.pdf

Watts, S. F. (2000). The mass budgets of carbonyl sulfide, dimethyl sulfide, carbon disulfide and hydrogen sulfide. *Atmospheric Environment*, *34*(5), 761–779. https://doi.org/10.1016/S1352-2310(99)00342-8

Wisthaler, A., Crawford, J.H., Haidahcer, S., Hanel, G., Hartungen, E., Jordan, A., … Sulzer, P. (2013). Development of a compact PTR-ToF-MS for suborbital research on the earth's atmospheric composition, In A Hansel & J. Dunkel (ed.), *6th International Conference on Proton Transfer Reaction Mass Spectrometry and its Applications. Contributions*. Innsbruck University Press.

Xu, X., Bingemer, H. G., Georgii, H.-W., Schmidt, U., & Bartell, U. (2001). Measurements of carbonyl sulfide (COS) in surface seawater and marine air, and estimates of the air-sea flux from observations during two Atlantic cruises. *Journal of Geophysical Research: Atmospheres*, *106*(D4), 3491–3502. https://doi.org/10.1029/2000JD900571

Zell, H. (2015, March 2). Earth's Atmospheric Layers [Text]. Retrieved November 12, 2016, from http://www.nasa.gov/mission_pages/sunearth/science/atmosphere-layers2.html

APPENDIX

Table A1. Surface can samples collected from previous SARP campaigns in 2009, 2012, 2014, and 2015 at various locations on the coast of California and on the Pacific Ocean. Includes location and carbonyl sulfide concentration for each sample.

Date	Latitude	Longitude	Location	OCS (pptv)
7/24/09	36° 36' 35.3" N	121° 53' 40.3" W	Monterey Bay, CA	551
7/24/09	n/a	n/a	Monterey Bay, CA	561
7/24/09	n/a	n/a	Monterey Coast	542
7/24/09	n/a	n/a	Monterey Coast	538
7/24/09	n/a	n/a	Monterey Coast	547
7/24/09	36° 36' 35.3" N	121° 53' 40.3" W	Monterey Bay, CA	560
7/25/09	35° 20' 7.2" N	120° 51' 45.3" W	Morro Bay, CA	587
7/5/12	34° 24’ 18” N	119° 51’ 48” W	Santa Barbara Channel	451
7/5/12	34° 24’ 8” N	119° 51’ 36” W	Santa Barbara Channel	436
7/5/12	34° 23’ 24” N	119° 54’ 36” W	Santa Barbara Channel	432
7/5/12	34° 24’ N	119° 53’ 24” W	Santa Barbara Channel	425
7/5/12	34° 23’ 11” N	119° 50’ 55” W	Santa Barbara Channel	448
6/25/14	34° 22’ 48” N	119° 42’ W	Santa Barbara Channel	518
6/25/14	34° 22’ 48” N	119° 42’ W	Santa Barbara Channel	529
6/25/14	34° 23’ 24” N	119° 43’ 48” W	Santa Barbara Channel	486
6/25/14	n/a	n/a	Santa Barbara Channel	498
6/25/14	34° 24' 39.5" N	119° 50' 52.2" W	UCSB NE of Lagoon	503
6/25/14	n/a	n/a	UCSB	498
6/25/14	34° 24' 22.0" N	119° 50' 36.3" W	Campus Point Beach, UCSB	525
6/11/15	36° 55' 36" N	121° 55' 54" W	Monterey Bay, CA	572
6/24/15	34° 22' 74" N	119° 43' 77" W	Santa Barbara Channel	582
6/24/15	34° 24' 38" N	119° 53' 28" W	Santa Barbara Channel	581
6/24/15	34° 23' 65" N	119° 43' 92" W	Santa Barbara Channel	544
6/24/15	34° 24' 21" N	119° 53' 43" W	Santa Barbara Channel	561
6/24/15	34° 27' 32" N	120° 3' 92" W	Santa Barbara Channel	532
6/25/15	34° 27’ 29” N	120° 1’ 22” W	Refugio State Beach	548
7/2/15	34° 24' 15" N	120° 13' 43" W	Gaviota State Beach	529
7/2/15	34° 24' 15" N	120° 13' 43" W	Gaviota State Beach	528
7/2/15	34° 25' 54" N	119° 55' 3" W	Haskell’s Beach	516
7/2/15	34° 28' 26" N	120° 8' 24" W	Santa Barbara Channel	514
7/2/15	34° 27' 37" N	120° 1' 40" W	El Capitan Beach	559
7/2/15	34° 27' 37" N	120° 1' 40" W	El Capitan Beach	551
7/2/15	34° 27' 31" N	120° 1' 28" W	El Capitan Beach	498
7/2/15	34° 25' 54" N	119° 55' 2" W	Haskell’s Beach	598
7/2/15	34° 24' 37" N	119° 52' 36" W	UCSB	556

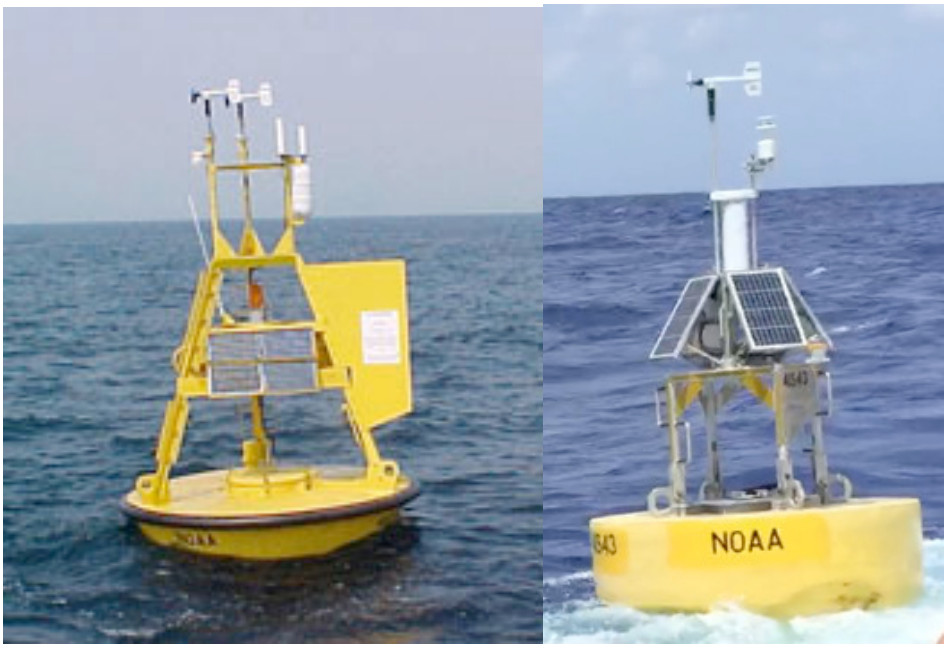

Figure A1. NOAA's buoy stations 46054 (left) and 46053 (right) located in the Santa Barbara Channel at 34°15'53" N 120°28'37" W (left) and 34°15'9" N 119°51'12" W (right).

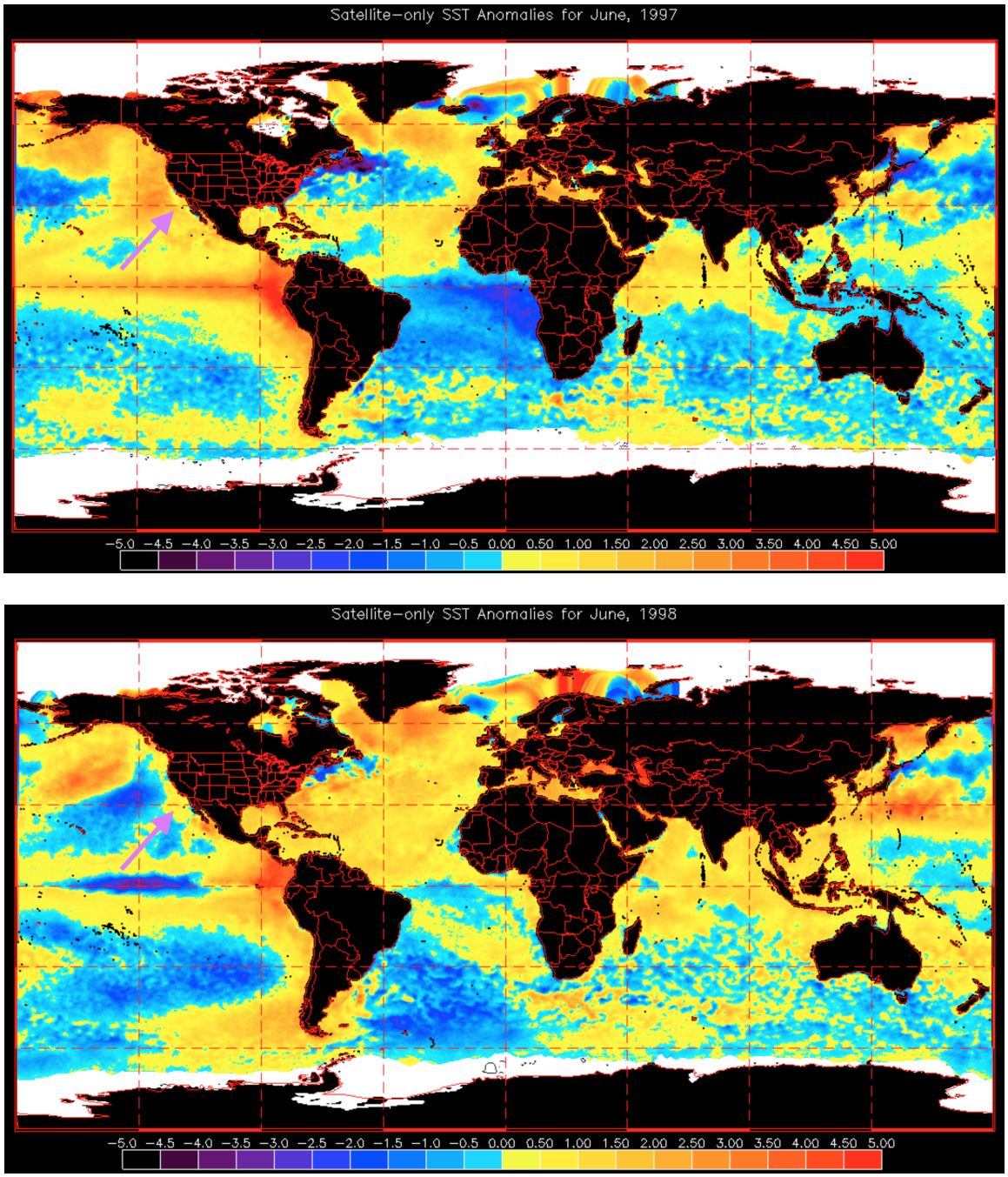

Figure A2. SST anomalies for June, 1997-1998 obtained from NOAA/NESDIS and highlighting the record-breaking El Niño event that brought higher than normal SST to California coast. Violet arrow distinguishing study region.

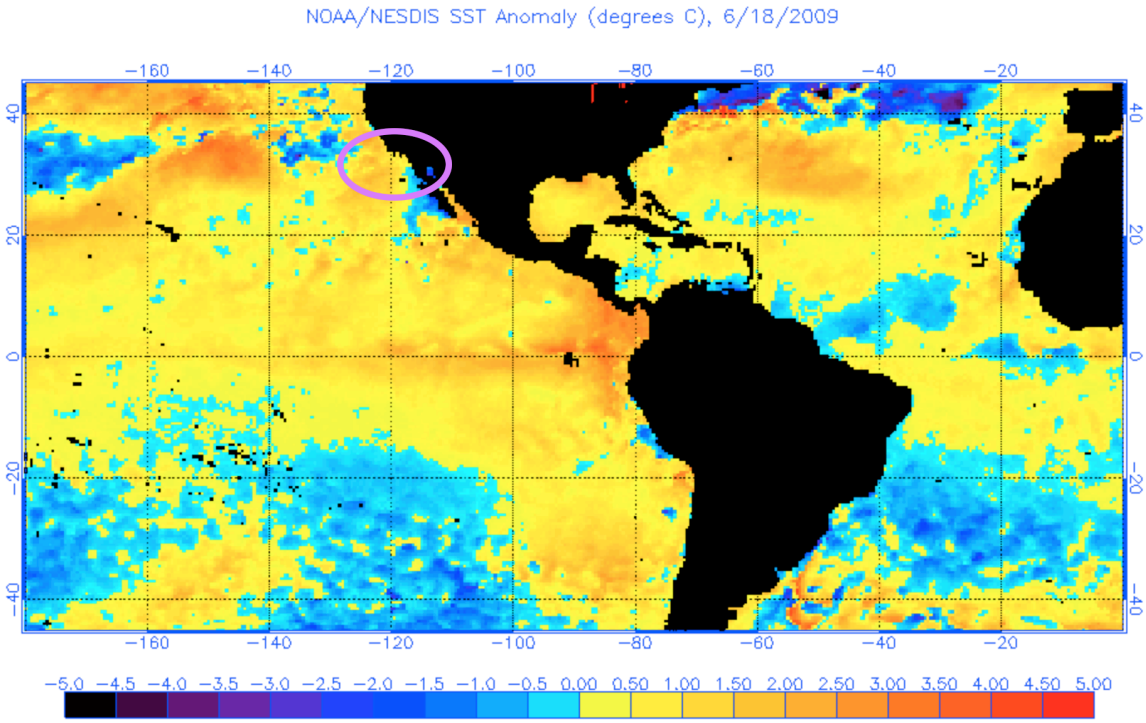

Figure A3. SST anomalies for June 18th, 2009 obtained from NOAA/NESDIS. Violet circle indicates study region.

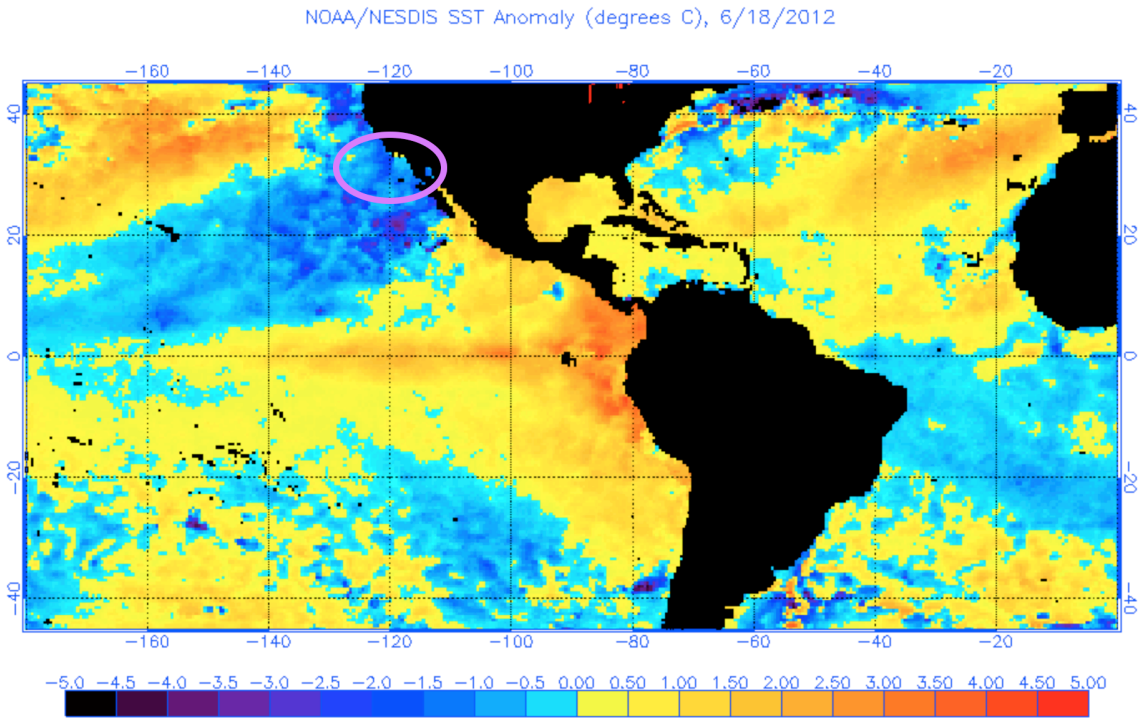

Figure A4. SST anomalies for June 18th, 2012 obtained from NOAA/NESDIS. Violet circle indicates study region.

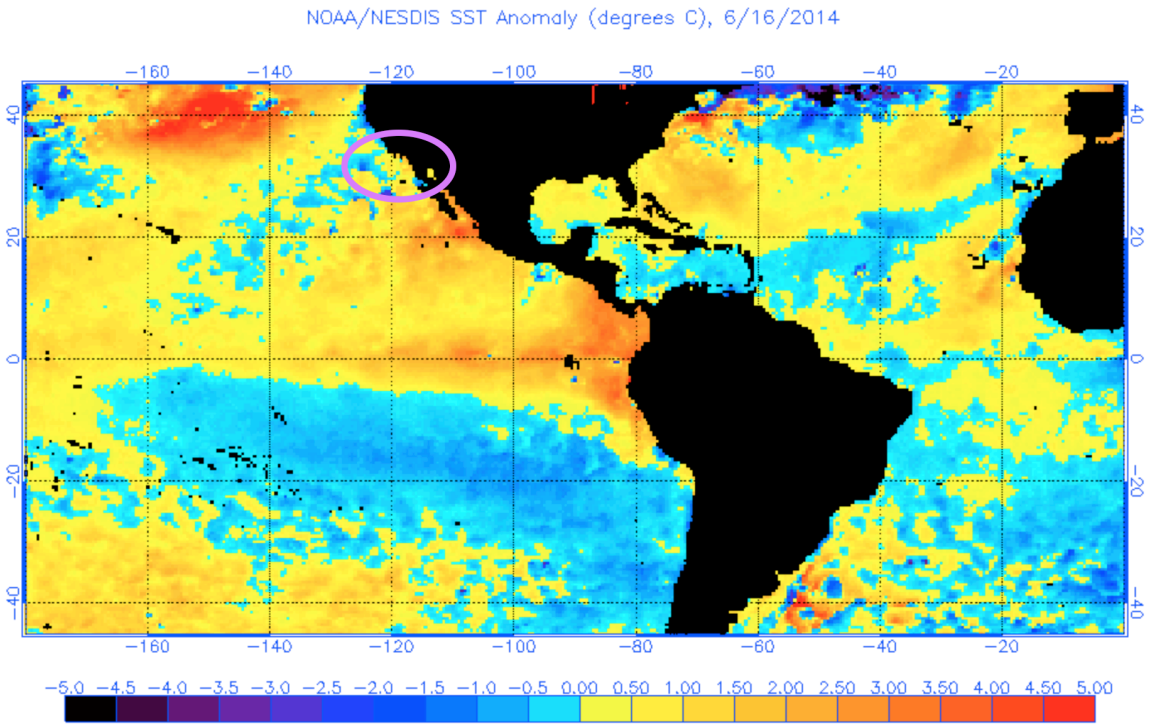

Figure A5. SST anomalies for June 16th, 2014 obtained from NOAA/NESDIS. Violet circle indicates study region.

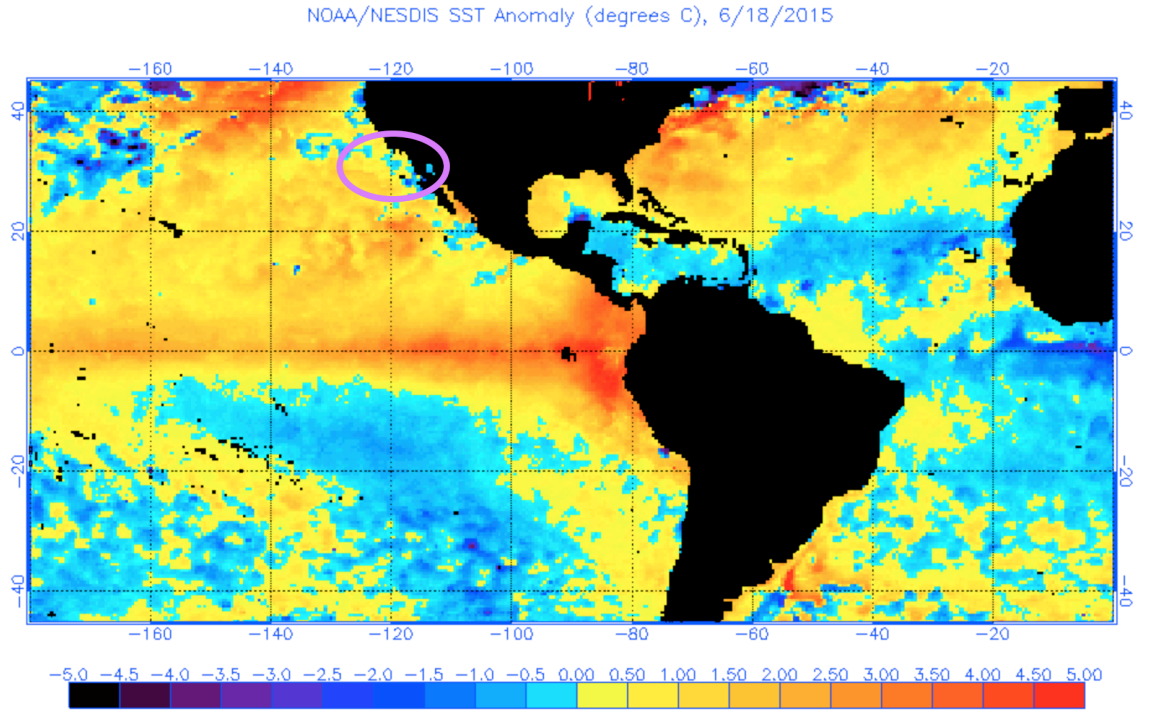

Figure A6. SST anomalies for June 18th, 2015 obtained from NOAA/NESDIS. Violet circle indicates study region.

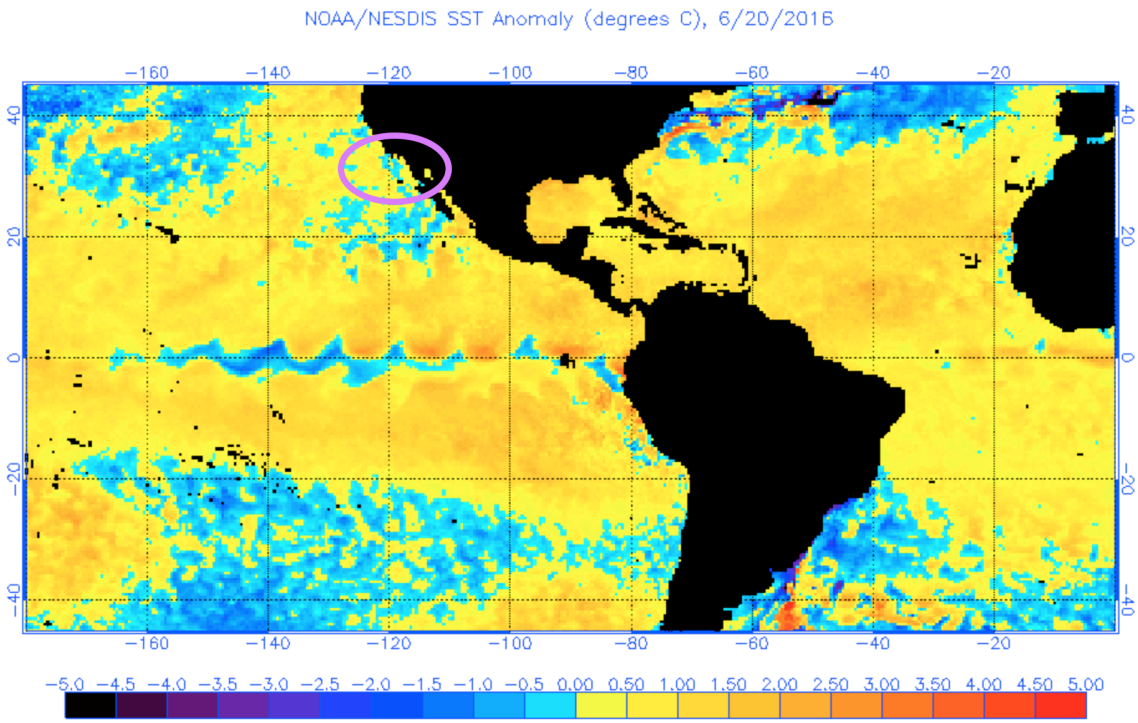

Figure A7. SST anomalies for June 20th, 2016 obtained from NOAA/NESDIS. Violet circle indicates study region.